Accepted Manuscript

Chalcophile elements in Martian meteorites indicate low sulfur content in the Martian interior and a volatile element-depleted late veneer

Zaicong Wang, Harry Becker

PII: S0012-821X(17)30035-3
DOI: http://dx.doi.org/10.1016/j.epsl.2017.01.023
Reference: EPSL 14287

To appear in: *Earth and Planetary Science Letters*

Received date: 26 August 2016
Revised date: 15 December 2016
Accepted date: 19 January 2017

Please cite this article in press as: Wang, Z., Becker, H. Chalcophile elements in Martian meteorites indicate low sulfur content in the Martian interior and a volatile element-depleted late veneer. *Earth Planet. Sci. Lett.* (2017), http://dx.doi.org/10.1016/j.epsl.2017.01.023

Highlights

- Ratios of Cu, S, Se, Te, Re, Pt and Pd in Martian meteorites are relatively constant.
- Martian meteorites show very limited eruptive losses of volatile Re, S, Se and Te.
- The parent magmas of most Martian meteorites were sulfide-undersaturated.
- Martian mantle and core have a low sulfur content.
- Low Te/PGE ratios in Martian meteorites reflect a strongly volatile element-depleted Martian late veneer.

Chalcophile elements in Martian meteorites indicate low sulfur content in the Martian interior and a volatile element-depleted late veneer

Zaicong Wang[a]* and Harry Becker[a]

[a]Freie Universität Berlin, Institut für Geologische Wissenschaften, Malteserstrasse 74-100, 12249 Berlin, Germany

*Correspondence to: Zaicong Wang, wzc231@163.com;

Current address: State Key Laboratory of Geological Processes and Mineral Resources, School of Earth Sciences, China University of Geosciences, 388 Lumo Road, Hongshan District, 430074, Wuhan, China

Abstract

It is generally believed that the Martian mantle and core are rich in sulfur and that shergottites originated from sulfide-saturated magma. However, recent work suggests that the high FeO contents would require very high S concentrations in shergottite parent magmas at sulfide saturation. Here we combine new and published data on chalcophile elements in shergottites, nakhlites and ALH84001 to constrain the sulfide saturation state of the parent magmas and the chalcophile element concentrations in their mantle sources.

Regardless of the MgO content and the long-term depletion history of incompatible lithophile elements as indicated by initial ε^{143}Nd, different groups of shergottites display limited variations in ratios of Pt, Pd, Re, Cu, S, Se and Te. The emplacement of most shergottites within the crust and limited variations of ratios of chalcophile elements with substantial differences in volatility during eruption (e.g., Cu/S, Cu/Se and Pt/Re) indicate little degassing losses of S, Se, Te and Re from shergottites. Limited variations in ratios of elements with very different sulfide-silicate melt partition coefficients and negative correlations of chalcophile elements with MgO require a sulfide-undersaturated evolution of the parent magmas from mantle source to emplacement in the crust, consistent with the FeO-based argument. Sulfide petrography and the komatiite-like fractionation of platinum group elements (PGE) in shergottites also support this conclusion. The absence of accumulated sulfides in the ancient Martian cumulate ALH8400l results in very low contents of PGE, Re, Cu, Se and Te in this meteorite, hinting that sulfide-undersaturated magmas may have occurred throughout the Martian geological history. The negative correlation of Cu and MgO contents in shergottites suggests approximately 2±0.4 (1s) μg/g Cu in the Martian mantle. The ratios of Cu, S, Se and Te indicate 360±120 μg/g (1s) S, 100±27 ng/g (1s) Se and 0.50±0.25 ng/g (1s) Te in the Martian mantle. At such low S concentrations, all S in Martian mantle sources may dissolve in basaltic melts that form at > 5 % partial melting.

Assuming equilibrium metal-silicate partitioning, and provided that the compositional model of the Martian mantle based on SNC meteorites is correct, Martian mantle inventories

of Cu, S and Se were mostly established by core formation and the Martian core should contain < 5-10 wt.% S only (depending on the choice of metal-silicate partition coefficients). The low S content in the Martian interior is consistent with the low Zn content in the Martian mantle, which indicates about 5 wt.% S in the core. In contrast, the highly siderophile PGE, Re and Te were added to the mantle by late accreted material after the Martian core formed. The near chondritic PGE ratios and the very low ratio of volatile Te to refractory PGE reflect a strongly volatile element-depleted late veneer and imply that the delivery of Martian water, presumably from carbonaceous chondrite like materials, must have occurred before accretion of the late veneer, likely within 2-3 million years after formation of the solar system.

Key words: sulfur, chalcophile elements, shergottite, Martian mantle, late veneer

1. Introduction

The sulfur content of the Martian mantle and the sulfide-saturation state of Martian magmas are key to constraining the S content in the core and its solidification history, the origin of its early magnetic field (Gaillard et al., 2013; Stevenson, 2001; Stewart et al., 2007), volcanic degassing and early evolution of the Martian surface-atmosphere system (Gaillard et al., 2013; King and McLennan, 2010; Righter et al., 2009). Based on accretion and core-mantle differentiation models, it is generally believed that the Martian interior is rich in sulfur, e.g., 10-16 wt.% S in the core and 100-2000 μg/g S in the mantle (Gaillard et al., 2013; Lodders and Fegley, 1997; Sanloup et al., 1999; Wänke and Dreibus, 1988). High S contents in Martian soils and widespread sulfate deposits (King and McLennan, 2010) were believed to result from either extensive degassing of S saturated magma (Righter et al., 2009) or weathering of sulfide-enriched basalts (Dehouck et al., 2012) .

Most Martian meteorites (the "SNC meteorites", shergottites, nakhlites, chassignites and the orthopyroxenite ALH84001) comprise of cumulate minerals with variable proportions of interstitial basaltic melt. The high FeO contents of Martian meteorites indicate that Martian basaltic magmas have high FeO contents. High FeO contents require S contents at sulfide saturation of > 2700-4300 μg/g, which is higher than S contents in most shergottites of 1000-3000 μg/g (Ding et al., 2014; Righter et al., 2009). The S contents in shergottites have been assumed to reflect losses of S induced by volcanic degassing of S-saturated magma (Righter et al., 2009) or, alternatively, to reflect sulfide-undersaturated conditions of the parent magmas of shergottites (Ding et al., 2015). A re-evaluation of the effect of high FeO contents and cumulus phases on S contents in shergottites suggests that melting of the mantle sources of shergottites may have led to sulfide-undersaturated magma and that the maximum S content in mantle sources of shergottites is 700-1000 μg/g (Ding et al., 2015).

The S content in the Martian mantle remains uncertain, because the S content of SNC meteorites may have been compromised by the possibility of degassing (Righter et al., 2009) and crustal contamination of some Martian magmas (Franz et al., 2014). Magmatic

fractionation of chalcophile elements with substantial differences in sulfide-silicate melt partition coefficients (e.g., Cu, Se, Te, Pd and other PGEs) represents another diagnostic indicator to distinguish sulfide-saturated from sulfide-undersaturated magmatic conditions.

To better constrain these important questions, we present new bulk rock Cu, S, Se and Te abundances in the same sample aliquot determined by isotope dilution ICP-MS in different groups of Martian meteorites. Contents of highly siderophile elements (HSE), Cu and S in SNC meteorites have been reported before, but Se and Te data are sparse and existing data show large uncertainties or variability (Lodders, 1998; Meyer, 2013; Wang et al., 1998; Smith et al., 1984; Treiman et al., 1986; Yang et al., 2015). Because of sample heterogeneity, particularly for chalcophile elements and limited quantities of available sample (e.g., Brandon et al., 2012; Ding et al., 2015; Yang et al., 2015), it is important to constrain their abundances and particularly element ratios in the same sample aliquot. Combined with published data, the abundances and ratios of chalcophile elements indicate a sulfide-undersaturated evolution of parent magmas of the SNC meteorites. The implications for a low S content in the Martian mantle and core and for accretion of a strongly volatile element-depleted late veneer on Mars will be discussed.

2. Samples and methods

2.1. Martian meteorites

We have obtained 0.2-0.25 gram-size fragments of 15 SNC meteorites (Table S1). Except for Sau 005, these samples are from falls and the cold desert of Antarctica, with limited terrestrial alteration. The meteorites consist of diverse groups: lherzolitic shergottites (ALHA77005, Y-000097), olivine-phyric shergottites (Sau 005, Y-980459, Tissint, EETA79001-A, LAR06319, LAR12011, LAR12095 and RBT04262), basaltic shergottite (Zagami), nakhlites (Y-000593, MIL03346, Nakhla) and orthopyroxenite cumulate ALH84001. Of these samples, Y-980459 and probably LAR06319 may represent closed-system

crystallization products of primitive magma from the Martian mantle (Basu Sarbadhikari et al., 2009; Mikouchi et al., 2004; Musselwhite et al., 2006; Usui et al., 2012).

These Martian meteorites show a range of petrological and geochemical characteristics with substantial differences in mantle source compositions (based on incompatible lithophile elements and Sr-Nd isotopes), magmatic evolution, oxygen fugacity and cover a large range of presumed formation ages from 4.1 Ga to 150 Ma (Table 1, Brandon et al., 2012; Herd et al., 2002; Lapen et al., 2010; Meyer, 2013; Mittlefehldt, 1994; Treiman, 2005; Wadhwa, 2008).

2.2. Analytical methods

Meteorite fragments were crushed using an agate mortar and processed to fine powder in a Retsch® oscillating ball mill MM 200 with agate cups. Before and after usage, the agate cups and mill were thoroughly cleaned by analytical-grade quartz sand and ethanol twice.

Bulk rock concentrations of Cu, S, Se and Te were determined on 0.1-0.15 gram sample powder aliquots by isotope dilution ICP-MS after digestion in concentrated HF-HNO_3 in Parr digestion bombs (190°C and 3 days). The details of the procedure have been described elsewhere and different geological reference materials and the replicates have produced reproducible results (typically <5%, 2 s.d., Wang et al., 2015). A brief outline of the method is given in Supplementary materials. Procedural blank corrections were always applied and negligible (<1 %) for S, Se and Cu, except for ALH84001 (Table 1). Because of the low Te abundances in SNC meteorites, blank corrections on Te were higher, commonly a few percent.

3. Results

The new data and their combined measurement uncertainties are listed in Table 1. ALH84001 has very low contents of Cu, Se and Te, which are only slightly higher than blank values. The S content of the meteorite (219 μg/g) is higher than the value (103 μg/g) reported in a previous study where $\Delta^{33}S$ data indicated that its S mainly reflects Martian crustal input (Franz et al., 2014).

Copper contents in the analyzed shergottites and nakhlites range from 2.7 to 10.6 μg/g, S from 311 μg/g to 3860 μg/g, Se from 74 to 585 ng/g and Te from 0.36 ng/g to 5.13 ng/g (Table 1). These elements in shergottites display broadly negative correlations with MgO contents (Figures 1 and S1). Nakhlites tend to have lower S, Se and Te contents relative to shergottites, except for MIL03346.

Although shergottites and nakhlites have variable contents of Cu, S, Se and Te, their ratios display less variation over the large range of MgO contents compared to terrestrial basalts and cumulate rocks (Variations are: < factor 2 for Cu/Se and factor 2-5 for Se/Te and Cu/Pd, Table 1, Figures 2-4; the mean ratios are Cu/Se = 20±4, Cu/Te = 4400±2000, Se/Te = 200±80 and Cu/Pd = 2650±950, uncertainties are 1s.d.). The relatively constant ratios compared to terrestrial basic magmatic rocks are independent of indicators of magmatic fractionation, radiogenic isotope compositions or incompatible lithophile element characteristics of Martian mantle sources (e.g., CI chondrite normalized $La/Yb_{(N)}$, initial $\varepsilon^{143}Nd$, Figures 5 and 6).

4. Discussion

4.1. The effect of Martian crustal contamination and terrestrial alteration

According to $\Delta^{33}S$ data, many Martian meteorites, particularly ALH 84001 and some nakhlites underwent variable extents of contamination by Martian crustal materials which have led to an increase in S contents (Franz et al., 2014). For instance, the S content of MIL03346 (3860 μg/g) is much higher than the S content of other SNC samples. Occasionally, S/Se ratios in some samples (e.g., MIL03346, RBT04262) are higher than the prevalent values (mean S/Se of 3600±800). These results are consistent with significant assimilation of Martian crustal sulfur by some of the parent magmas (Franz et al., 2014).

Although Martian crustal contamination has affected S abundances in ALH84001, the very low Cu, Se, Te, Re and PGE contents indicate negligible addition of these elements during contamination with Martian crust (this work and Jones et al., 2003). Samples with severe contamination by Martian crustal S (e.g., MIL03346 and RBT04262) display no obvious

differences in Cu contents and in ratios of Cu, Se and Te, compared to less contaminated samples. These results indicate a limited effect of Martian crustal contamination on the ratios of these elements in these samples (except for an increase of S/Se). Minor effects of Martian crustal contamination that cannot be resolved by S isotopic compositions or S/Se are included in the variance of the means of element ratios in Table 1. Terrestrial weathering of meteorites often results in the loss of sulfur (e.g., Huber et al., 2006), however, the hot desert sample Sau 005 shows similar ratios of Cu, S, Se and Te as other Martian meteorites, implying limited effects of terrestrial alteration on these elements in this sample.

4.2. Sample heterogeneity and chalcophile element ratios

Overall, the new S, Se and Cu contents are within the range of literature data and sometimes show different values compared to previous work for the same samples (Figures 1-3, Table S2). It has been shown that because the predominant host phase of chalcophile elements are trace sulfide phases (Lorand and Luguet, 2016), concentrations obtained on different aliquots of the same sample may vary substantially, e.g., S, Cu and the HSE (Brandon et al., 2012; Ding et al., 2015; Jones et al., 2003; Meyer, 2013; Yang et al., 2015). Literature data suggest rather low Te contents in shergottites and nakhlites, at the level of a few ng/g or less, close to the detection limit of radiochemical neutron activation analysis (e.g., Smith et al., 1984; Treiman et al., 1986; Wang et al., 1998, Table S2). Tellurium contents of the present study display similar, but sometimes lower values (Figure 2, Table S2), due to the lower detection limit of the isotope dilution method, which is mainly controlled by procedural blanks. The scatter of chalcophile element concentrations reflects different precision and accuracy of the applied methods and particularly sample heterogeneity, i.e., the heterogeneous distribution of fine-grained sulfides at relatively small sample sizes used for analyses.

Provided that abundances of different chalcophile elements are obtained from the same digestion aliquots of samples, the effect of sample heterogeneity on *element ratios* should be limited. Thus in the following discussion we use element ratios wherever possible to constrain fractionation of chalcophile elements. The Cu, S, Se and Te data in this study were determined

by isotope dilution-ICP-MS methods on the same digestion aliquots. The same is true for the HSE concentration data in Brandon et al. (2012). Another study has applied laser ablation ICP-MS to obtain bulk rock HSE, Cu, S, Se and Te data on shergottites (Yang et al., 2015). Unfortunately, the detection limits in the latter work were high for some critical elements (e.g., 18 ng/g for Pd, 100 ng/g for Se and 35 ng/g for Te). Some literature data on Se and Te contents were from the same sample aliquots with Se/Te ratios showing a range similar to ours (e.g., Smith et al., 1984; Treiman et al., 1986; Wang et al., 1998, Table S2). These data indicate low Te contents in Martian meteorites.

4.3. Limited effects of degassing on chalcophile elements in shergottites

In terrestrial submarine basaltic volcanics that erupted on the seafloor at substantial water depth, degassing did not affect the concentrations of S, Se, Te and Re (Lissner et al., 2014; Norman et al., 2004; Sun et al., 2003; Yi et al., 2000). In contrast, subaerial counterparts tend to have lower S, Se, Te and Re contents, indicating their degassing due to their volatile character during volcanic eruptions in these environments. Among these elements, S is commonly the most volatile element during degassing of basic magmas (Greenland and Aruscavage, 1986; Norman et al., 2004; Yi et al., 2000). Thus it is necessary to first evaluate the effect of possible degassing on these elements in shergottites.

The parameters affecting volcanic degassing are primarily pressure of emission, pre-eruptive fO_2 and the initial water content in the melt (Gaillard and Scaillet, 2009). In general, the lower the emission pressure, the more oxidized and/or the more water rich, the more S is degassed from the melt. In the case of hypothetical Martian basalts with 500 μg/g water, 3500 μg/g S and fO_2 of QFM -3.5 to -1, sulfur is almost not lost by degassing at pressures > 5 bar (Gaillard and Scaillet, 2009). Lherzolitic, olivine-phyric and basaltic shergottites contain variable amounts of cumulus phases and were emplaced at variable depth, but mostly not at subaerial pressures. For instance, saturation with olivine and pyroxene in olivine-phyric shergottite Y980459 was estimated to have occurred at 12 kbar (Musselwhite et al., 2006). The

emplacement within various levels of the crust suggests that most Martian meteorites underwent no or only little degassing of S.

Sulfur, Se and Te have significantly different volatilities during volcanic degassing with S being commonly more volatile than Se and the latter more volatile than Te (Greenland and Aruscavage, 1986; Jenner et al., 2010; Lissner et al., 2014; Rubin, 1997). The ratios of these elements relative to the non-volatile elements Cu and the PGE provide further constraints on the limited effect of degassing on these elements in the shergottites. Copper is not volatile during degassing of subaerially erupted basic magmas (Norman et al., 2004). Degassed shergottites should display increasing Cu/Se with increasing extent of degassing relative to the ratios of EETA79001, Y980459 and lherzolitic shergottites which are samples crystallized at depth (e.g., Musselwhite et al., 2006). As is obvious from Figures 2 and 3, shergottites show less than a factor of 2 variation in Cu/Se, with a mean Cu/Se of most shergottites within ± 30% uncertainty. The uncertainty includes the effect of possible degassing, if relevant, on the mean Cu/Se. Except for samples with obvious sulfur input from Martian crustal contamination (e.g., MIL03346 and RBT04262), S/Se and Cu/S in most lherzolitic, olivine-phyric and basaltic shergottites vary within a limited range. Because S is much more volatile than Se and Cu (Jenner et al., 2010), the ratios of S/Se and Cu/S are consistent with limited degassing of S (which should substantially decrease S/Se and increase Cu/S, if strong and variable degassing occurred). Cu/Te and Se/Te ratios in shergottites show larger variations by a factor of 2-4. In terrestrial magmas, Te is less volatile than Se (Greenland and Aruscavage, 1986; Lissner et al., 2014; Rubin, 1997). This may indicate that the larger variations of Cu/Te and Se/Te may not have been caused by degassing, but probably by other processes. Finally, it has been shown that significant fractions of Re may be lost along with S by degassing during subaerial eruption of arc and Hawaiian basaltic and picritic magmas (Norman et al., 2004; Sun et al., 2003). We note that the ratios of Re to Pd and Pt in different groups of shergottites are also relatively constant (Brandon et al., 2012), further supporting the limited effect of degassing on the SNC meteorites.

Consequently, parent magmas of shergottites display no clear evidence for volatility-related losses of S, Se, Te and Re. Most sulfides in lherzolitic, olivine-phyric and basaltic shergottites show homogenous and nearly chondritic ^{34}S (Franz et al., 2014). The absence of mass dependent fractionation of ^{34}S in these shergottites is consistent with little or no degassing of the parent magmas of these meteorites.

Some nakhlites show evidence from quench textures for degassing (Chevrier et al 2011), however, if this affected the abundances of chalcophile elements is unclear. Degassing losses of S in some nakhlites cannot be excluded (see S-MgO diagram, Figure S1), however, Se and Te in the melt phase trapped in the studied nakhlites are high because the nakhlites lie on a common mixing line between augite and a melt endmember (Figure S1). The calculated Se contents (500-600 ng/g) of the parental magmas of nakhlites lie on the trend defined by the shergottites, which argues for small losses of Se by degassing from these samples. For Te, the calculated melt composition is about 3-4 ng/g, which is lower than shergottite parent magma compositions extrapolated to similar MgO (Figure S1). The scattered behavior of Te may reflect mantle heterogeneity, which is also indicated by the scatter of the shergottite data. Because the data on nakhlites are limited to a few samples, future work needs to confirm these interpretations.

4.4. Sulfide saturation state of Martian magmas

4.4.1. Sulfide-undersaturated parent magmas of the shergottites

Copper, Se, Te and Pd show substantial differences in sulfide-silicate melt partition coefficients, e.g., $D^{\text{sulfide-silicate}}_{Se}$ (200-1500) < $D^{\text{sulfide-silicate}}_{Cu}$ (500-1600) < $D^{\text{sulfide-silicate}}_{Te}$ (2500-10000) < $D^{\text{sulfide-silicate}}_{Pd}$ (10^5-10^6) (e.g., Brenan, 2015; Mungall and Brenan, 2014; Patten et al., 2013). Many factors affect partition coefficients and complete sulfide-silicate melt equilibration is not necessarily ascertained in natural processes (e.g., Becker and Dale, 2016; Wang and Becker, 2015a). Nevertheless, the relative bulk partitioning behavior of these elements can be predicted based on natural samples and experimentally determined partition coefficients, e.g., D_{Te}/D_{Se} of 5-9 and D_{Te}/D_{Cu} of 2-10 at 3-22wt.% FeO in the silicate melt and $D_{Cu} << D_{Pd}$ (Brenan,

2015; Mungall and Brenan, 2014; Patten et al., 2013; Wang and Becker, 2015a). These data indicate that sulfide saturation and segregation would lead to large variations of ratios of these elements with magmatic fractionation (e.g., Cu/Te, Se/Te and particularly Cu/Pd, Figures 3 and 4). This is the case in sulfide-saturated terrestrial basaltic magmas such as MORB, gabbros from the Oman ophiolite and mantle pyroxenites (Jenner et al., 2010, 2012; Lissner et al., 2014; Patten et al., 2013; Peucker-Ehrenbrink et al., 2012; Wang and Becker, 2015a).

If magmas are sulfide-undersaturated during partial melting and fractional crystallization, Cu, Se, Te, Pt and Pd should mostly partition into silicate melt, provided that no other platinum group minerals are exsolved during the high-temperature evolution of magmas (Given the estimated temperatures during the formation of Martian magmas and the stability of tellurides this is considered unlikely (Helmy et al., 2007). The stability of Pt-Ir and other PGE alloy phases will be discussed below). Melting and fractional crystallization of silicates and spinel would affect the bulk contents of these elements, but not their *ratios*, because these processes result in *concurrent* enrichment of these elements in derivative melts and dilution in mixtures of cumulate phases and interstitial melt until they evolve to late stage sulfide saturation (e.g., terrestrial komatiites, olivine-phyric shergottites, nakhlites, Figures 4, 6 and S2). This behavior is very different from the behavior of these elements during sulfide-saturated conditions.

Like in sulfide undersaturated komatiites, contents of Cu, Se and Pd in most shergottites show negative correlations with MgO (e.g., Figures 1 and S1). Cu/Pd ratios have only a factor of 3-4 variations (mean Cu/Pd = 2650±950, 1s.d.) over a large range of MgO contents, a very different behavior compared to the three orders of magnitude variation of Cu/Pd in MORB and terrestrial gabbros (Figure 4). The relatively constant Cu/Pd ratios require sulfide-undersaturated conditions during partial melting and fractional crystallization of parent magmas of shergottites. Otherwise, residual sulfides during mantle melting and sulfide saturation during magmatic evolution would fractionate these elements and lead to much larger variations in Cu/Pd ratios as in most terrestrial counterparts (a factor of hundreds, Figure 4). The contents and ratios of the HSE in shergottites further support sulfide-undersaturated

magmatic evolution. At sulfide-undersaturated conditions like in komatiites, Os-Ir-Ru become enriched in early magmatic cumulate phases such as silicates and alloys and behave as compatible elements; whereas Pd, Re and Pt become enriched in the melt, like incompatible lithophile elements (e.g., Barnes and Fiorentini, 2008; Brenan et al., 2016; Puchtel et al., 2009). This process would lead to fractionation of compatible Os-Ir-Ru from incompatible Pt-Pd-Re, but with relatively constant Os/Ir, Pt/Pd and Pt/Re ratios (Figure 6). Exactly this is what the HSE data of shergottites show (Brandon et al., 2012).

Most sulfides in shergottites occur as tiny grains, located near rims of pyroxenes or in interstitial mesostasis, intimately intergrown with Fe-Ti oxides (King and McLennan, 2010; Lorand et al., 2005). These observations suggest that sulfide precipitation in shergottites occurred only at a very late stage during the cooling of interstitial melt (Lorand et al., 2005), consistent with sulfide under-saturation of the parent magma.

4.4.2. Long-term history of sulfide-undersaturated conditions?

It is unclear if the ancient magmas that erupted before the deposition of S on the Martian surface at 3.0-3.7 Ga (Carr and Head, 2010) were also sulfide-undersaturated. The orthopyroxenite cumulate ALH84001 likely crystallized at ~ 4.1 Ga and is characterized by very low Re and PGE contents (Jones, 2003). These data were previously interpreted to reflect early stage sulfide-saturation which had removed all PGE (Righter et al., 2015). Our new data show that ALH84001 also has very low contents of Cu, Se and Te, whereas sulfur concentrations are higher because of later crustal contamination (Franz et al., 2014). Copper and particularly Se are only slightly more chalcophile than S (Brenan, 2015; Wang and Becker, 2015a; and references therein). These compositions suggest that no sulfide precipitation occurred during orthopyroxene accumulation, as would be the case for sulfide-undersaturated parent magma compositions. Sulfide-saturation of the parent magma of ALH84001 likely would have led to precipitation of magmatic sulfide in the orthopyroxene cumulate, which would have enriched less chalcophile elements such as Re, Cu and Se contents even if PGE contents were low.

The average S content on the Martian surface environment was estimated to 1-3 wt.% (King and McLennan, 2010) and a conservative estimate of total surficial SO_3 in Martian soil, sedimentary deposits and polar sulfates comprises about 7.5×10^{16} kg (Righter et al., 2009). This budget accounts for only 0.06 µg/g S in bulk silicate Mars (assuming a mass of 5×10^{23} kg, about 80 wt.% of bulk Mars, Lodders and Fegley, 1997; Wänke and Dreibus, 1988). Even if the surficial sulfate budget was 10 times more, it is still negligible compared to the mantle. It is difficult to constrain the S content of the primordial Martian crust. Considering that most Martian meteorites were derived from deeper levels of the Martian crust as reflected by the crystallization of cumulus minerals, the range of 0.1 to 0.3 wt.% S in Martian meteorites may provide an approximate estimate. These data hint that any S transfer from mantle to the crust during Mars' geological history likely had a negligible effect on the budget of S and other chalcophile elements in the mantle. The shergottites formed much later than the sulfate deposits of the surface, yet the chondritic $\delta^{34}S$ of sulfides in shergottites (Franz et al., 2014) indicates no significant transfer of sulfur between the mantle and the crust. Thus, based on mass balance, current data suggest a limited influence of the Martian crust on element and isotopic budgets of S in the Martian mantle. Therefore, sulfide-undersaturated conditions may represent a secular feature of magma derived from the Martian mantle.

4.5. Composition of chalcophile elements in the Martian mantle

Because of the magmatic evolution at sulfide-undersaturated conditions and limited losses by degassing during emplacement of the parent magmas, ratios of the incompatible chalcophile elements Cu, S, Se, Te, Pd and Pt in Martian meteorites should reflect the parent magma compositions. If during mantle melting sulfide liquid is not retained in the mantle source, chalcophile element ratios in parent magmas of shergottites also reflect those of the mantle sources and thus, mantle compositions of chalcophile elements can be determined.

Whether or not sulfides are retained in the mantle during melting depends on the S content of the mantle, the degree of partial melting, the P-T path during melting and the sulfur content of melts at sulfide saturation (e.g., Ding et al., 2015). About 10-30 % partial melting of

a primitive Martian mantle composition can explain most SNC parent magmas and surface basalts (except for Martian alkaline magma suites, Collinet et al., 2015). The shergottites typically formed from depleted or incompatible element-enriched mantle sources and require relatively high degrees of partial melting, e.g., 15% melting for Tissint (e.g., Humayun et al., 2013). At maximum S contents of 700-1000 μg/g in the Martian mantle, >17% partial melting would produce sulfide-undersaturated primitive magma (Ding et al., 2015). If the S content is lower, e.g. 360 μg/g as in the present study (see below), mantle sulfides in the SNC magma sources (Estimated temperature 1450 ± 70°C, Filiberto and Dasgupta, 2015) would have been consumed at > 5% melting, a degree much lower than those estimated for mantle sources of shergottites (Ding et al., 2015).

4.5.1. Ratios of incompatible chalcophile elements in Martian mantle sources

Compositional variations in shergottites originated either from variable degrees of melting of different mantle sources or from variable crustal contamination (Jones, 2015 and references therein). In spite of the large differences, mostly reflected in major element compositions and incompatible lithophile elements and radiogenic isotopes, the ratios of incompatible elements Pt, Pd, Re, Cu, Te and Se in different shergottites show relatively small variations, independent of mantle sources and magmatic evolution of the parent magmas. For example, Cu/Se and Pt/Pd ratios in shergottites with enriched, intermediate and depleted lithophile element isotopic signatures vary by a factor of 2 only (Figures 2 and 6). The variation of Pd/Pt ratios in shergottites from chondritic to suprachondritic ratios (Figure 6 and Brandon et al., 2012) may reflect the stability of Pt alloys in the Martian mantle or in the sulfide-undersaturated magmas as a function of the degree of partial melting, magmatic evolution and fO_2 (Brenan et al., 2016; Mungall and Brenan, 2014). Cu/Pd and Se/Te ratios show a similar behavior, albeit with somewhat larger variations by a factor of 2-5 (Figures 2-5). These features indicate restricted variations in ratios of incompatible chalcophile elements in the different mantle sources relative to incompatible lithophile elements.

Nakhlites formed at ~ 1.3 Ga and have mantle source compositions and a magmatic fractionation history that differs from shergottites (Treiman, 2005). Some nakhlites underwent strong crustal assimilation and incorporated significant proportions of sulfur from Martian surface environments (Chevrier et al., 2011; Franz et al., 2014). We note that Cu/Te and Se/Te in Y-000593 and MIL03346 are similar to values in shergottites, but Nakhla (6.03 μg/g Cu) has higher Cu/Se and Cu/Te ratios (Figures 2-3). These complexities and the limited data make it difficult to interpret the currently available chalcophile element data on nakhlites.

4.5.2. Cu, S, Se and Te contents in the Martian mantle

The Cu content of 2.0 ± 0.4 μg/g (1s) in the Martian mantle has been calculated from the negative correlation with MgO at 29-33 wt.% MgO, the most likely range of concentrations in the Martian mantle (Taylor, 2013). Considering possible effects of sample heterogeneity or analytical uncertainty of different data sets on the estimated Cu content, the Cu-MgO correlation was reassessed by only using the values of shergottites from the present study (n=11) for comparison (Figure 1). The Cu-MgO correlation of shergottites also passes through element abundances of shergottite olivine cumulates (e.g., 33-35 wt.% MgO, Yang et al., 2015), similar to in terrestrial komatiites that are also used to estimate mantle source compositions (Puchtel et al., 2016; Puchtel et al., 2009). This behavior indicates that it is viable to use the Cu-MgO correlation of shergottites to estimate the Cu content of their mantle sources. The isotope dilution data yields the same result as Taylor (2013), indicating that a Cu content of 2.0±0.4 μg/g is a robust estimate. The scatter of the correlation includes the effects of heterogeneities inherited from the diversity of mantle sources of shergottites.

The mantle contents of S, Se and Te can be estimated from their ratios relative to Cu. We have calculated the ratios using the new data (Table 1). Samples Y-980459 and LAR06319, putative primitive magma compositions from the Martian mantle offer an alternative way to support our estimates of the mantle source composition. Ratios of Cu, Se and Te in LAR06319 are similar to the mean values of shergottites and nakhlites. Ratios of Cu, S and Se of Y-980459 are within the scatter of the data, also similar to the mean values.

Because some previous concentration data are afflicted with poorly known uncertainties (e.g., Te) and are not from the same sample aliquots, they were not included in calculation of the mean values. The estimated S, Se and Te contents in the Martian mantle are listed in Table 2. For example, Cu/Se is 20±4 (n=12), resulting in a Se content of 100±27 ng/g, similar to 85±18 ng/g based on Se/Yb (Taylor, 2013). Cu/Te and Se/Te ratios are 4400±2000 and 200±80 (n=12), respectively. Previous RNAA data on Se and Te contents show Se/Te of 60-330, with a mean of 180±110, similar to our new data (Smith et al., 1984; Treiman et al., 1986; Wang et al., 1998; Table S2). Thus, the Martian mantle has a low Te content of 0.50±0.25 ng/g. Sample Y-980459 has the lowest Cu/Te and Se/Te of this study and yields a provisional maximum of 1.5 ng/g Te in the Martian mantle.

S/Cu and S/Se ratios can be used to constrain the S concentration in the Martian mantle, which has not been well constrained before. Crustal contamination can elevate S contents in Martian meteorites (Franz et al., 2014) and thus would affect S/Cu and S/Se ratios (e.g., MIL03346 and RBT04262). LAR06319 also seems to have incorporated crustal S by post-crystallization alteration as revealed by $\Delta^{33}S$ data (Franz et al., 2014) and this is also shown by its high S/Se ratio of 5300. Other analyzed samples show relatively constant and lower S/Se ratios, implying low levels of contamination with crustal S. The mean S/Se of 3600±800 (n=11) should be regarded as a maximum value for the Martian mantle and suggests that the Martian mantle contains only 360±120 µg/g S. The S/Cu ratio of 170±65 in these samples yields a similar maximum S of 340±140 µg/g.

S/Se ratios of different groups of chondrites are rather constant, with a mean value of 2500±400 (Dreibus et al., 1995; Wang and Becker, 2013; and references therein). Thus, because of the cosmochemical similarity of S and Se, the mean chondritic value represents a reasonable estimate for S/Se in bulk Mars. Metal-silicate melt partition coefficients of S and Se are very similar at P-T conditions relevant for Martian core formation with Se showing slightly more preference for metal compared to S (Rose-Weston et al., 2009). Because core formation may have led to only a slight increase of the S/Se in the mantle compared to in the bulk planet, the slightly chondritic S/Se ratio of 3600±800 may be representative of the Martian mantle.

Therefore, the consistent data place improved constraints on the S composition of the Martian mantle.

4.6. Composition of the Martian late veneer

Most Martian meteorites show chondritic Os/Ir, Pt/Pd, Pt/Re and Re/Os (indicated by approximately chondritic $^{187}Os/^{188}Os$, Brandon et al., 2012; Dale et al., 2012; Day et al., 2016; Jones et al., 2003). Recently, HSE abundances in the Martian mantle were interpreted to be consistent with metal-silicate partitioning at 14±3 GPa based on experimental results at 1.5 GPa and 1400°C (Righter et al., 2015). However, Mann et al (2012) and Laurenz et al (2016) presented HSE partitioning results at higher P-T conditions (6-21 GPa and > 2200°C), which have covered the conditions of Martian core-mantle fractionation without any extrapolation. They also evaluated the effect of S in the metal. These results indicate strong fractionation of the HSE during Martian core formation. Therefore, the chondritic HSE ratios in Martian mantle are difficult to explain by core formation. Instead, the chondritic ratios of the HSE suggest that like for Earth's mantle, the Martian mantle also received late accreted material after core formation was complete (e.g., Brandon et al., 2012; Dale et al., 2012; Day et al., 2016).

The abundances of highly siderophile elements in the Martian mantle have been estimated mainly by HSE-MgO correlations (Day et al., 2016; Taylor, 2013) and co-variation of HSE (Dale et al., 2012). These two different approaches have led to similar Pt and Pd contents but relatively large differences in the estimates for Os, Ir and Ru abundances in the Martian mantle (Day et al., 2016). The evolution of Martian magma under sulfide-undersaturated conditions permits an alternative way to assess the HSE contents in the Martian mantle and the fraction of the Martian late veneer.

At sulfide-undersaturated conditions, Pd, Pt and Re behave as incompatible elements. Following the approach for Cu, variations with MgO may constrain mantle abundances of these HSE. Using samples with MgO contents ≥ 15% suggests abundances of Pt and Pd in the Martian mantle of 3.1±0.8 ng/g and 2.4±0.8 ng/g, respectively (Taylor, 2013). Shergottites yield a mean Cu/Pd of 2650±950 (n=14, Figure 4, higher than that calculated from Cu and Pd contents). This

value leads to 1.0±0.7 ng/g Pd in the Martian mantle, slightly lower than other estimates. Abundances of compatible HSE like Os, Ir and Ru in the Martian mantle can be estimated by assuming chondritic HSE ratios based on Pt and Pt contents. These values are approximately equivalent to $0.3^{+0.1}_{-0.2}$% of the mass of Mars if the late accreted material had a CI chondritic HSE composition (Figure 7).

4.6.1. A strongly volatile element-depleted Martian late veneer

The addition of late accreted material may also have affected the moderately volatile elements Cu, S, Se and Te. The contribution of the late veneer to the volatile element inventory of the Martian mantle cannot exceed the contents of these elements in the Martian mantle. Because the Te content in the Martian mantle is rather low (< 1.5 ng/g, a mean at 0.5±0.25 ng/g, 1s), the CI chondrite-normalized ratio of volatile Te relative to refractory Pt or Ir in Martian mantle is 0.06. This value is lower than the ratios in most chondrites (Wang and Becker, 2013; Wasson and Kallemeyn, 1988). Only the strongly volatile element-depleted H chondrites display similar Te depletion and its relative pattern is shown for comparison in Figure 7. The low Te/HSE ratio in the Martian mantle indicates that the Martian late veneer was strongly depleted in Te and likely also other volatile elements. It is unclear if the late veneer originated from chondritic materials or from other materials that were even more strongly depleted in volatile elements than known chondrites. We note that the compositional spectrum of volatile element fractionation and depletion in early solar system objects may be different from that observed in chondrite parent bodies from the asteroid belt (e.g., Wang et al., 2016).

The CI chondrite-normalized Cu/Ir, Se/Ir and S/Ir ratios of the Martian mantle are 4.1±0.8, 1.31±0.35 and 1.85±0.62, respectively. Because these values are higher than in CI chondrite, the predominant fraction of Cu, S and Se in the Martian mantle was inherited from metal-silicate partitioning during core formation (Figure 7). Figures 7 and 8 show the combined effects of Martian core formation and late accretion of primitive material. The former led to moderate depletion of Cu, S and Se and strong depletion of the HSE and Te, and the latter delivered the excess in the HSE, but nearly no Te and likely little Cu, Se and S. This explanation

484 is fully consistent with the metal-silicate partitioning data of these elements at relevant P-T-fO_2
485 for Martian core formation (Rai and van Westrenen, 2013; Righter and Chabot, 2011).

486 Tellurium is always more siderophile and chalcophile relative to S and Se, both at low
487 and high pressure-temperature conditions (Brenan, 2015; Rose-Weston et al., 2009). In contrast,
488 metal-sulfide-silicate melt fractionation of S from Se during core formation is limited. For
489 example, experiments at 8-19 GPa and 2000-2420 °C at fO_2 (ΔIW) of -0.42 to -1.89, show log
490 D_{Te} of 2.5 to 3.5 and log $D_{Se} \geq$ log D_S of 1.8 to 2.7 (Rose-Weston et al., 2009), where D is the
491 liquid metal-liquid silicate partition coefficient. This means that core-mantle fractionation with
492 or without sulfide segregation into the core would lead to a depletion of Te relative to S and Se
493 by at least a factor of 5-6. The slightly supra-chondritic S/Se and highly supra-chondritic S/Te
494 and Se/Te in the Martian mantle are consistent with a predominant control of this ratio in the
495 Martian mantle by metal segregation, which extracted S and Se to a similar and moderate extent
496 but almost all Te (Rose-Weston et al., 2009). The subsequent delivery of a strongly volatile-
497 element depleted Martian late veneer added only little Te, Cu, Se and S.

498 **4.6.2. Comparison of chalcophile elements in the Martian and terrestrial mantle**

499 Earth is a larger planet than Mars and has a much higher Cu content in the mantle than
500 Mars (Figure 7, Wang and Becker, 2015b; references therein). This difference is consistent with
501 experiment constraints that Cu becomes less siderophile with increasing P-T conditions of core
502 formation (e.g., Corgne et al., 2008). At the high P-T conditions of core formation relevant to
503 Earth, S, Se and Te become more siderophile (Rose-Weston et al., 2009). Accordingly, if the
504 Te concentration in Earth's mantle was only affected by core formation and not by late accretion,
505 high P-T core formation would have yielded a mantle with even lower Te than in the Martian
506 mantle. However, Earth's mantle has a much higher Te content (about 11 ng/g, Wang and
507 Becker, 2013) than the Martian mantle and CI chondritic ratios of S, Se and Te. This
508 composition cannot be explained by core formation. It requires late additions of relative volatile
509 element-rich primitive material (Wang and Becker, 2013). If half (Labidi et al., 2013) or all
510 (Boujibar et al., 2014) of the S content of Earth's mantle were inherited from the main accretion

stage of the Earth rather than delivered by late accretion, this would have led to highly suprachondritic S/Te and Se/Te in Earth's mantle, similar to the Martian mantle prior to late accretion.

Consequently, the significant differences in Cu, S, Se and Te abundances in model compositions of Earth's and the Martian mantle in combination with approximately chondritic HSE ratios further strengthens the importance of late accretion and the different volatile element compositions of material accreted late onto Mars and the Earth, strongly volatile element-depleted on Mars, and volatile element-rich on Earth.

4.6.3. Implications for the origin of Martian water and carbon

The strongly volatile element-depleted late veneer provides a critical constraint on the timing of the delivery of water and carbon on Mars. Hydrogen isotopes have indicated that Martian water originated from carbonaceous chondrite like materials rather than comets (Usui et al., 2012). If the Martian late veneer was strongly volatile element-depleted, it cannot have delivered substantial quantities of water and carbon. This constraint indicates that the delivery of Martian water must have occurred before the late veneer (Figure 8), and thus not later than the cessation of core formation, perhaps within 2-3 Ma after formation of the solar system (e.g., Dauphas and Pourmand, 2011). The new results support the view that the delivery of water to Mars, Vesta, Earth and the Moon by accretion of volatile-rich materials occurred over a period from a few Ma to 100 Ma. At least on Mars and Vesta, and presumably also on the Earth, water was retained during early planetary impacts and growth (Sarafian et al., 2014).

4.7. Low sulfur content in the Martian core?

It is possible to constrain the S content in the Martian core by using the S content in the mantle and metal-silicate partition coefficients at the relevant P-T-fO_2 conditions. Abundances of moderately siderophile elements in the Martian mantle are consistent with metal-silicate equilibration at mean pressures and temperatures of 14 ± 3 GPa and 2100 ± 200 K, respectively (Rai and van Westrenen, 2013; Righter and Chabot, 2011; Yang et al., 2015). Experimentally-determined $D_S^{metal\text{-}silicate}$ at conditions relevant for Martian core formation are less than 200 (see

summary in Boujibar et al. 2014), e.g, $D_S^{metal\text{-}silicate}$ of 80 at 16 GPa, 2200 °C and fO_2 (ΔIW) of -1.79 (experiment #29) (Boujibar et al., 2014) and around 200 at 15 GPa, 2000-2300 °C and fO_2 (ΔIW) of -1.56 (run number of BGI-N) (Rose-Weston et al., 2009). These partition coefficients should be regarded as upper bounds for Martian core formation because of the possible presence of other elements in the metal and lower fO_2 of core formation, which both significantly reduce $D_S^{metal\text{-}silicate}$ (Boujibar et al., 2014). If the Martian core formed at disequilibrium conditions during multi-stage accretion, apparent $D_S^{metal\text{-}silicate}$ also would be lower, and thus the S content in the Martian core would also be lower. Different accretion models have indicated that a planetary mantle with 200 µg/g S may have been in equilibrium with a core containing 2 wt.% S only (bulk $D_S^{metal\text{-}silicate}$ of 100), even at high P-T conditions relevant for Earth (Boujibar et al., 2014). Because of the strongly decreasing siderophile affinity of S with decreasing pressure (Boujibar et al., 2014), the smaller size of Mars suggests that $D_S^{metal\text{-}silicate}$ during Martian core formation must have been lower than for Earth.

Because the high FeO contents in the Martian mantle and in mantle-derived magmas require a very high sulfur content at sulfide saturation at pressures < 15 GPa (Ding et al., 2014; Laurenz et al., 2016), e.g., > 2000 µg/g for Martian mantle at 14±3 GPa (Ding et al., 2014), it is rather unlikely that segregation of FeS ("sulfide matte") occurred during Martian core formation. Segregation of FeS would require > 2000 µg/g S in the Martian mantle, which is not supported by data on SNC meteorites.

Thus, if the S contents of the mantle sources of SNC parent magmas estimated in the present study are representative of the Martian mantle, the S content in the Martian core should be less than 10 wt. % (assuming upper bounds: 480 µg/g, $D^{metal\text{-}silicate}_S$ < 200), lower than previously assumed values of 10-25 wt.% (Khan and Connolly, 2008; Lodders and Fegley, 1997; Wänke and Dreibus, 1988). The specific S content in the Martian core depends on the details of core formation conditions and history. A few wt.% S in the Martian core is consistent with constraints from the Zn abundance of 60-70 µg/g in the Martian mantle (Lodders and Fegley, 1997; Yang et al., 2015), which is only slightly higher than Zn in Earth's mantle. Zinc is essentially lithophile (Wang et al. 2016 and references therein) and has a similar volatility as

S (Dreibus and Palme, 1996). The similar volatility of Zn and S indicates < 5 wt. % S in the Martian core (Note that based on volatility arguments, Gaillard and Scaillet (2009) estimated around 3 wt.% S in the core).

A low S content in Martian core, if confirmed, may require a reassessment of models for the evolution of the physical state of the Martian core (Stewart et al., 2007), the core density or other light elements in the Martian core, the viability of an early geodynamo, and the origin and transient occurrence of the magnetic field that shielded the early atmosphere and liquid water on the early Martian surface from the solar wind (Stevenson, 2001).

5. Conclusions

Precise new data of Cu, S, Se and Te abundances in Martian meteorites of diverse origins and magmatic evolution, combined with literature data indicate that the mantle-derived parent magmas of Martian meteorites were sulfide-undersaturated. Various arguments that include the size of the crustal sulfur reservoir, chondritic $\delta^{34}S$ in sulfides of shergottites and very low contents of most chalcophile elements in the ancient Martian sample ALH84001 suggest that sulfide-undersaturated conditions prevailed over Martian geological history. Sulfide-undersaturated conditions during mantle melting and magmatic evolution led to limited variations of ratios of the incompatible chalcophile elements Pt, Pd, Re, Cu, S, Se and Te in Martian meteorites. Ratios of these elements and correlations with MgO content constrain their mantle contents, of which S content is only 360±120 μg/g (1s). Due to their high FeO content, primitive Martian magmas formed at more than a few percent partial melting would have dissolved all sulfide in Martian mantle sources, regardless of their history of lithophile incompatible element enrichment or depletion.

Martian mantle inventories of Cu, S and Se were mostly established by core formation. Metal-silicate partitioning data suggest that the Martian core likely contains a few percent of S only. A low sulfur content in the Martian mantle and core is consistent with the low Zn abundance in the Martian mantle. The very low ratio of volatile Te to refractory PGE reflects a

strongly volatile element-depleted Martian late veneer and implies that the delivery of Martian water must have occurred before accretion of the late veneer, likely within 2-3 million years after formation of the solar system. Comparison of mantle contents of Cu, S, Se, Te and the approximately chondritic HSE ratios of Mars and Earth indicates the importance of late accretion and the different volatile element compositions of late accreted material on Mars and Earth.

Acknowledgements: Special thanks to the providers of Martian meteorites (Meteorite Working Group, ANSMET and the Smithsonian Institution, USA; Antarctic Meteorite Research Center, NIPR, Japan; C. Smith, Natural History Museum, UK; J. Zipfel, Senckenberg Institute, Frankfurt am Main, Germany). We thank M. Feth and P. Gleissner for technical support and several anonymous reviewers for constructive and critical comments on the manuscript. This work was supported by DFG funding (Be1820/12-1 and SFB-TRR 170 Subproject B1). This is TRR 170 Publication No. 3.

606 **Figure captions**

607 Figure 1. Variation of Cu contents of Martian meteorites with MgO contents. Overall, Cu and
608 MgO in different groups of shergottites show a broadly negative correlation ([Cu] μg/g = -0.42
609 * [MgO] wt.% + 14.9, R^2=0.80, n=12, including olivine in shergottites). The estimated Cu
610 content of the Martian mantle is from Taylor (2013) and confirmed by our new data. Multiple
611 analyses of the same sample in the literature (Meyer, 2013) and the new data occasionally show
612 variable Cu contents (dashed lines indicate samples where large differences have been reported),
613 indicating the effect of sample heterogeneity on Cu abundances. Copper contents in three
614 olivines from shergottites measured by laser ablation ICP-MS in Yang et al (2015) were 3-7
615 μg/g or below the detect limit of 0.1 μg/g. Considering the low Cu content in ALH 84001 and
616 the low bulk rock abundances of Cu in most shergottites, olivine should have very low Cu
617 contents. Thus olivine is assumed to have low Cu contents of < 0.1 μg/g.
618
619 Figure 2. Variations of Cu, S, Se and Te contents in Martian meteorites. Literature data are
620 shown for comparison (Lodders, 1998; Meyer, 2013; Wang et al., 1998; Table S2). Note that
621 the estimated Cu, S, Se and Te contents in the Martian mantle are from this study (Data in this
622 and the following figures from Table 2).
623
624 Figure 3. Variation of ratios of Cu, S, Se and Te in Martian meteorites with MgO contents.
625 These element ratios display limited variations for most samples, including different groups of
626 shergottites and nakhlites (except Nakhla). The behavior of the shergottite data differ from the
627 evolution trend of sulfide saturated terrestrial MORB (Jenner and O'Neill, 2012; Lissner et al.,
628 2014) and terrestrial cumulate rocks (Wang and Becker, 2015a), which show strong
629 fractionation of Cu, Se and Te because of different sulfide-silicate melt partition coefficients
630 (Te > Cu > Se ≥ S). S/Se ratios change little during melting and fractional crystallization of
631 basalts, even if sulfide saturation was attained (Jenner and O'Neill, 2012; Wang and Becker,
632 2015a). Occasionally high S/Se ratios in Martian meteorites (e.g., RBT04262, MIL03346 and
633 LAR06319) reflect assimilation of S from the Martian crust. Blue bands are the ranges of ratios

(±1s) in most of the analyzed meteorites (Table 1). Differences between data from the present study and literature data for individual meteorites (Meyer, 2013; Smith et al., 1984; Treiman et al., 1986; Wang et al., 1998; Table S2) are indicated by the dashed line. Error bars (1s) are shown for the new data and most errors are smaller than symbol sizes.

Figure 4. Cu/Pd ratios in shergottites and in terrestrial mantle-derived magmatic rocks. Because sulfide-silicate melt partition coefficients of Cu (~10^3) and Pd (~10^5-10^6) are very different (Mungall and Brenan, 2014), sulfide saturation and segregation during fractional crystallization leads to highly variable Cu/Pd in evolving melts and cumulates, e.g., up to 3 orders of magnitude in lower crustal gabbros (Peucker-Ehrenbrink et al., 2012) and in MORB glasses (e.g., Lissner et al., 2014). In contrast, terrestrial komatiites from Victoria's lava lake (Puchtel et al., 2016) display constant Cu/Pd in rocks that display a range of MgO contents. Note Cu/Pd ratios of these komatiites overlap Cu/Pd of Earth's mantle, indicating that the Cu/Pd ratio of sulfide-undersaturated magma generally reflects its mantle source. As in terrestrial komatiites, Cu/Pd in most shergottites are relatively constant (2650±950, blue band) over a large range of MgO contents, consistent with sulfide-undersaturated magmatic evolution. Literature Pd contents in shergottites are from Brandon et al (2012), and the corresponding Cu contents are from this study and Meyer (2013). Because of sample heterogeneity, literature data on Y-980459 and Dhofar 019 display highly variable PGE contents and thus Cu data obtained on different aliquots yield apparently different Cu/Pd (gray symbols with dashed lines). The Pd value of a replicate of Dhofar 019 is from Jones et al. (2003) whereas a lower Pd content for Y-980459 was measured by Yang et al. (2015). Because Cu and Pd contents are not from the same sample aliquots, this contributes to the scatter of Cu/Pd ratios (a factor of 3-4 variation).

Figure 5. Ratios of Cu/Se versus CI chondrite normalized $La/Yb_{(N)}$ and $\varepsilon^{143}Nd_{initial}$, respectively. a) Shergottites and some nakhlites (except Nakhla) have similar Cu/Se ratios. Data source from Table 1. b) Shergottites from different mantle sources show relatively constant Cu/Se ratios. $\varepsilon^{143}Nd_{initial}$ data sources are given in Table 1. The original references are listed in the supplement.

Figure 6. Fractionation of ratios of Pt and Pd with Ir in different groups of shergottites. The strong fractionation of Pd/Ir and Pt/Ir by three orders of magnitude, but limited fractionation of Pt/Pd indicates sulfide-undersaturated magmatic evolution (a). Lherzolitic shergottites have Pt/Pd similar to CI chondrites, whereas olivine-phyric and basaltic shergottites display a mean Pt/Pd of 0.84, which is slightly lower than the value of CI chondrites (a). Pd/Pt ratios show limited variations of less than a factor of 3 in depleted, intermediate and enriched shergottites (b). Data from Brandon et al. (2012).

Figure 7. CI chondrite normalized abundances of S, Se, Te, Cu and highly siderophile elements in the mantles of Mars and Earth (This study; Becker et al., 2006; Lodders, 2003; Taylor, 2013; Wang and Becker, 2013). The Martian mantle is strongly depleted in Te, which yields a maximum value for the contribution of Te from metal-silicate partitioning during core formation. This value also indicates late accretion of a strongly volatile element-depleted late veneer on Mars. In contrast, Cu, S and Se in the Martian mantle are primarily left over from metal-silicate segregation. Among chondrites, H chondrites (a) have the lowest Te/Ir and Te/Se ratios (Wasson and Kallemeyn, 1988). The pattern b) represents an alternative composition of volatile element-depleted late accreted material with ratios of volatile elements similar to CI chondrites.

Figure 8. Schematic depiction of the final stages of core formation on Mars and Earth and subsequent late accretion. Sulfur, Se and Te in the mantle of Earth and Mars in combination with approximately chondritic HSE ratios require late accretion of volatile element-depleted and -undepleted material onto Mars (this work) and Earth (Wang and Becker, 2013), respectively. The final stages of Martian core formation occurred much earlier (e.g., Dauphas and Pourmand, 2011) than on Earth (Jacobson et al., 2014). The ‘dry’ Martian late veneer implies that the Martian water was delivered before the late veneer. See text for details.

References

Barnes, S.J., Fiorentini, M.L., 2008. Iridium, ruthenium and rhodium in komatiites: Evidence for iridium alloy saturation. Chem. Geol. 257, 44-58.

Basu Sarbadhikari, A., Day, J.M.D., Liu, Y., Rumble Iii, D., Taylor, L.A., 2009. Petrogenesis of olivine-phyric shergottite Larkman Nunatak 06319: Implications for enriched components in martian basalts. Geochimica et Cosmochimica Acta 73, 2190-2214.

Becker, H., Dale, C.W., 2016. Re–Pt–Os Isotopic and Highly Siderophile Element Behavior in Oceanic and Continental Mantle Tectonites. Rev. Mineral. Geochem. 81, 369-440.

Becker, H., Horan, M.F., Walker, R.J., Gao, S., Lorand, J.-P., Rudnick, R.L., 2006. Highly siderophile element composition of the Earth's primitive upper mantle: Constraints from new data on peridotite massifs and xenoliths. Geochim. Cosmochim. Acta 70, 4528-4550.

Boujibar, A., Andrault, D., Bouhifd, M.A., Bolfan-Casanova, N., Devidal, J.-L., Trcera, N., 2014. Metal–silicate partitioning of sulphur, new experimental and thermodynamic constraints on planetary accretion. Earth Planet. Sci. Lett. 391, 42-54.

Brandon, A.D., Puchtel, I.S., Walker, R.J., Day, J.M.D., Irving, A.J., Taylor, L.A., 2012. Evolution of the martian mantle inferred from the (187)Re-(187)Os isotope and highly siderophile element abundance systematics of shergottite meteorites. Geochimica Et Cosmochimica Acta 76, 206-235.

Brenan, J.M., 2015. Se–Te fractionation by sulfide–silicate melt partitioning: Implications for the composition of mantle-derived magmas and their melting residues. Earth Planet. Sci. Lett. 422, 45-57.

Brenan, J.M., Bennett, N.R., Zajacz, Z., 2016. Experimental Results on Fractionation of the Highly Siderophile Elements (HSE) at Variable Pressures and Temperatures during Planetary and Magmatic Differentiation. Rev. Mineral. Geochem. 81, 1-87.

Carr, M.H., Head, J.W., III, 2010. Geologic history of Mars. Earth Planet. Sci. Lett. 294, 185-203.

Chevrier, V., Lorand, J.-P., Sautter, V., 2011. Sulfide petrology of four nakhlites: Northwest Africa 817, Northwest Africa 998, Nakhla, and Governador Valadares. Meteoritics & Planetary Science 46, 769-784.

Collinet, M., Médard, E., Charlier, B., Vander Auwera, J., Grove, T.L., 2015. Melting of the primitive martian mantle at 0.5–2.2 GPa and the origin of basalts and alkaline rocks on Mars. Earth and Planetary Science Letters 427, 83-94.

Corgne, A., Keshav, S., Wood, B.J., McDonough, W.F., Fei, Y.W., 2008. Metal-silicate partitioning and constraints on core composition and oxygen fugacity during Earth accretion. Geochim. Cosmochim. Acta 72, 574-589.

Dale, C.W., Burton, K.W., Greenwood, R.C., Gannoun, A., Wade, J., Wood, B.J., Pearson, D.G., 2012. Late Accretion on the Earliest Planetesimals Revealed by the Highly Siderophile Elements. Science 336, 72-75.

Dauphas, N., Pourmand, A., 2011. Hf-W-Th evidence for rapid growth of Mars and its status as a planetary embryo. Nature 473, 489-492.

732 Day, J.M.D., Brandon, A.D., Walker, R.J., 2016. Highly Siderophile Elements in Earth, Mars,
733 the Moon, and Asteroids. Rev. Mineral. Geochem. 81, 161-238.

734 Debaille, V., Brandon, A.D., O'Neill, C., Yin, Q.Z., Jacobsen, B., 2009. Early martian mantle
735 overturn inferred from isotopic composition of nakhlite meteorites. Nature Geoscience 2, 548-
736 552.

737 Dehouck, E., Chevrier, V., Gaudin, A., Mangold, N., Mathé, P.E., Rochette, P., 2012.
738 Evaluating the role of sulfide-weathering in the formation of sulfates or carbonates on Mars.
739 Geochim. Cosmochim. Acta 90, 47-63.

740 Ding, S., Dasgupta, R., Lee, C.-T.A., Wadhwa, M., 2015. New bulk sulfur measurements of
741 Martian meteorites and modeling the fate of sulfur during melting and crystallization –
742 Implications for sulfur transfer from Martian mantle to crust–atmosphere system. Earth and
743 Planetary Science Letters 409, 157-167.

744 Ding, S., Dasgupta, R., Tsuno, K., 2014. Sulfur concentration of martian basalts at sulfide
745 saturation at high pressures and temperatures – Implications for deep sulfur cycle on Mars.
746 Geochimica et Cosmochimica Acta 131, 227-246.

747 Dreibus, G., Palme, H., 1996. Cosmochemical constraints on the sulfur content in the Earth's
748 core. Geochim. Cosmochim. Acta 60, 1125-1130.

749 Dreibus, G., Palme, H., Spettel, B., Zipfel, J., Wänke, H., 1995. Sulfur and selenium in
750 chondritic meteorites. Meteoritics 30, 439-445.

751 Franz, H.B., Kim, S.-T., Farquhar, J., Day, J.M.D., Economos, R.C., McKeegan, K.D., Schmitt,
752 A.K., Irving, A.J., Hoek, J., Iii, J.D., 2014. Isotopic links between atmospheric chemistry and
753 the deep sulphur cycle on Mars. Nature 508, 364-368.

754 Filiberto, J., Dasgupta, R., 2015. Constraints on the depth and thermal vigor of melting in the
755 Martian mantle. Journal of Geophysical Research: Planets 120, 109-122.

756 Gaillard, F., Michalski, J., Berger, G., McLennan, S.M., Scaillet, B., 2013. Geochemical
757 Reservoirs and Timing of Sulfur Cycling on Mars. Space Science Reviews 174, 251-300.

758 Gaillard, F., Scaillet, B., 2009. The sulfur content of volcanic gases on Mars. Earth and
759 Planetary Science Letters 279, 34-43.

760 Greenland, L.P., Aruscavage, P., 1986. Volcanic emission of Se, Te, and As from Kilauea
761 volcano, Hawaii. J. Volcanol. Geotherm. Res. 27, 195-201.

762 Helmy, H.M., Ballhaus, C., Berndt, J., Bocrath, C., Wohlgemuth-Ueberwasser, C., 2007.
763 Formation of Pt, Pd and Ni tellurides: experiments in sulfide-telluride systems. Contrib. Mineral.
764 Petrol. 153, 577-591.

765 Herd, C.D.K., Borg, L.E., Jones, J.H., Papike, J.J., 2002. Oxygen fugacity and geochemical
766 variations in the martian basalts: implications for martian basalt petrogenesis and the oxidation
767 state of the upper mantle of Mars. Geochimica et Cosmochimica Acta 66, 2025-2036.

768 Huber, H., Rubin, A.E., Kallemeyn, G.W., Wasson, J.T., 2006. Siderophile-element anomalies
769 in CK carbonaceous chondrites: Implications for parent-body aqueous alteration and terrestrial
770 weathering of sulfides. Geochim. Cosmochim. Acta 70, 4019-4037.

771 Humayun, M., Nemchin, A., Zanda, B., Hewins, R.H., Grange, M., Kennedy, A., Lorand, J.P.,
772 Gopel, C., Fieni, C., Pont, S., Deldicque, D., 2013. Origin and age of the earliest Martian crust
773 from meteorite NWA 7533. Nature 503, 513-516.

774 Jacobson, S.A., Morbidelli, A., Raymond, S.N., O'Brien, D.P., Walsh, K.J., Rubie, D.C., 2014.
775 Highly siderophile elements in Earth/'s mantle as a clock for the Moon-forming impact. Nature
776 508, 84-87.

777 Jenner, F.E., Arculus, R.J., Mavrogenes, J.A., Dyriw, N.J., Nebel, O., Hauri, E.H., 2012.
778 Chalcophile element systematics in volcanic glasses from the northwestern Lau Basin.
779 Geochem. Geophys. Geosyst. 13, Q06014, doi:06010.01029/02012GC004088.

780 Jenner, F.E., O'Neill, H.S.C., 2012. Analysis of 60 elements in 616 ocean floor basaltic glasses.
781 Geochem. Geophys. Geosyst. 13, Q02005, doi:02010.01029/02011GC004009.

782 Jenner, F.E., O'Neill, H.S.C., Arculus, R.J., Mavrogenes, J.A., 2010. The magnetite crisis in
783 the evolution of arc-related magmas and the initial concentration of Au, Ag and Cu. J. Petrol.
784 51, 2445-2464.

785 Jones, J.H., 2015. Various aspects of the petrogenesis of the Martian shergottite meteorites.
786 Meteoritics & Planetary Science 50, 674-690.

787 Jones, J.H., Neal, C.R., Ely, J.C., 2003. Signatures of the highly siderophile elements in the
788 SNC meteorites and Mars: a review and petrologic synthesis. Chem. Geol. 196, 21-41.

789 Khan, A., Connolly, J.A.D., 2008. Constraining the composition and thermal state of Mars from
790 inversion of geophysical data. Journal of Geophysical Research: Planets 113, E07003.

791 King, P.L., McLennan, S.M., 2010. Sulfur on Mars. Elements 6, 107-112.

792 Labidi, J., Cartigny, P., Moreira, M., 2013. Non-chondritic sulphur isotope composition of the
793 terrestrial mantle. Nature 501, 208-211.

794 Lapen, T.J., Righter, M., Brandon, A.D., Debaille, V., Beard, B.L., Shafer, J.T., Peslier, A.H.,
795 2010. A Younger Age for ALH84001 and Its Geochemical Link to Shergottite Sources in Mars.
796 Science 328, 347-351.

797 Laurenz, V., Rubie, D.C., Frost, D.J., Vogel, A.K., 2016. The importance of sulfur for the
798 behaviour of highly-siderophile elements during Earth's differentiation. Geochim. Cosmochim.
799 Acta 194, 123-138.

800 Lissner, M., König, S., Luguet, A., le Roux, P.J., Schuth, S., Heuser, A., le Roex, A.P., 2014.
801 Selenium and tellurium systematics in MORBs from the southern Mid-Atlantic Ridge (47–
802 50°S). Geochim. Cosmochim. Acta 144, 379-402.

803 Lodders, K., 1998. A survey of shergottite, nakhlite and chassigny meteorites whole-rock
804 compositions. Meteoritics & Planetary Science 33, A183-A190.

805 Lodders, K., 2003. Solar system abundances and condensation temperatures of the elements.
806 Astrophys. J. 591, 1220-1247.

807 Lodders, K., Fegley, B., 1997. An oxygen isotope model for the composition of Mars. Icarus
808 126, 373-394.

809 Lorand, J.-P., Luguet, A., 2016. Chalcophile and siderophile elements in mantle rocks: trace
810 elements controlled by trace minerals. Rev. Mineral. Geochem. 81, 441-488.

811 Lorand, J.P., Chevrier, V., Sautter, V., 2005. Sulfide mineralogy and redox conditions in some
812 shergottites. Meteoritics & Planetary Science 40, 1257-1272.

Mann, U., Frost, D.J., Rubie, D.C., Becker, H., Audetat, A., 2012. Partitioning of Ru, Rh, Pd, Re, Ir and Pt between liquid metal and silicate at high pressures and high temperatures - Implications for the origin of highly siderophile element concentrations in the Earth's mantle. Geochim. Cosmochim. Acta 84, 593-613.

Meyer, C., 2013. The Martian Meteorite Compendium. Astromaterials Research & Exploration Science (ARES), http://curator.jsc.nasa.gov/antmet/mmc/.

Mikouchi, T., Koizumi, E., McKay, G., Monkawa, A., Ueda, Y., Chokai, J., Miyamoto, M., 2004. Yamato 980459: mineralogy and petrology of a new shergottite-related rock from Antarctica. Antarctic meteorite research 17, 13.

Mittlefehldt, D.W., 1994. ALH84001, a cumulate orthopyroxenite member of the martian meteorite clan. Meteoritics 29, 214-221.

Mungall, J.E., Brenan, J.M., 2014. Partitioning of platinum-group elements and Au between sulfide liquid and basalt and the origins of mantle-crust fractionation of the chalcophile elements. Geochim. Cosmochim. Acta 125, 265-289.

Musselwhite, D.S., Dalton, H.A., Kiefer, W.S., Treiman, A.H., 2006. Experimental petrology of the basaltic shergottite Yamato-980459: Implications for the thermal structure of the Martian mantle. Meteoritics & Planetary Science 41, 1271-1290.

Norman, M.D., Garcia, M.O., Bennett, V.C., 2004. Rhenium and chalcophile elements in basaltic glasses from Ko'olau and Moloka'i volcanoes: Magmatic outgassing and composition of the Hawaiian plume1. Geochim. Cosmochim. Acta 68, 3761-3777.

Patten, C., Barnes, S.-J., Mathez, E.A., Jenner, F.E., 2013. Partition coefficients of chalcophile elements between sulfide and silicate melts and the early crystallization history of sulfide liquid: LA-ICP-MS analysis of MORB sulfide droplets. Chem. Geol. 358, 170-188.

Peucker-Ehrenbrink, B., Hanghoj, K., Atwood, T., Kelemen, P.B., 2012. Rhenium-osmium isotope systematics and platinum group element concentrations in oceanic crust. Geology 40, 199-202.

Puchtel, I.S., Touboul, M., Blichert-Toft, J., Walker, R.J., Brandon, A.D., Nicklas, R.W., Kulikov, V.S., Samsonov, A.V., 2016. Lithophile and siderophile element systematics of Earth's mantle at the Archean-Proterozoic boundary: Evidence from 2.4 Ga komatiites. Geochim. Cosmochim. Acta 180, 227–255.

Puchtel, I.S., Walker, R.J., Brandon, A.D., Nisbet, E.G., 2009. Pt-Re-Os and Sm-Nd isotope and HSE and REE systematics of the 2.7 Ga Belingwe and Abitibi komatiites. Geochim. Cosmochim. Acta 73, 6367-6389.

Rai, N., van Westrenen, W., 2013. Core-mantle differentiation in Mars. Journal of Geophysical Research-Planets 118, 1195-1203.

Righter, K., Chabot, N.L., 2011. Moderately and slightly siderophile element constraints on the depth and extent of melting in early Mars. Meteoritics & Planetary Science 46, 157-176.

Righter, K., Danielson, L.R., Pando, K.M., Williams, J., Humayun, M., Hervig, R.L., Sharp, T.G., 2015. Highly siderophile element (HSE) abundances in the mantle of Mars are due to core formation at high pressure and temperature. Meteoritics & Planetary Science 50, 604-631.

Righter, K., Pando, K., Danielson, L.R., 2009. Experimental evidence for sulfur-rich martian magmas: Implications for volcanism and surficial sulfur sources. Earth Planet. Sci. Lett. 288, 235-243.

856 Rose-Weston, L., Brenan, J.M., Fei, Y.W., Secco, R.A., Frost, D.J., 2009. Effect of pressure,
857 temperature, and oxygen fugacity on the metal-silicate partitioning of Te, Se, and S:
858 Implications for earth differentiation. Geochim. Cosmochim. Acta 73, 4598-4615.

859 Rubin, K., 1997. Degassing of metals and metalloids from erupting seamount and mid-ocean
860 ridge volcanoes: Observations and predictions. Geochim. Cosmochim. Acta 61, 3525-3542.

861 Sanloup, C., Jambon, A., Gillet, P., 1999. A simple chondritic model of Mars. Phys. Earth
862 Planet. Inter. 112, 43-54.

863 Sarafian, A.R., Nielsen, S.G., Marschall, H.R., McCubbin, F.M., Monteleone, B.D., 2014.
864 Early accretion of water in the inner solar system from a carbonaceous chondrite–like source.
865 Science 346, 623-626.

866 Shirai, N., Ebihara, M., 2009. Chemical characteristics of the lherzolitic shergottite Yamato
867 000097: magmatism on Mars inferred from the chemical compositions of shergottites. Polar
868 Science 3, 117-133.

869 Smith, M.R., Laul, J.C., Ma, M.S., Huston, T., Verkouteren, R.M., Lipschutz, M.E., Schmitt,
870 R.A., 1984. Petrogenesis of the SNC (shergottites, nakhlites, chassignites) meteorites:
871 Implications for their origin from a large dynamic planet, possibly Mars. Journal of Geophysical
872 Research: Solid Earth 89, B612-B630.

873 Stevenson, D.J., 2001. Mars' core and magnetism. Nature 412, 214-219.

874 Stewart, A.J., Schmidt, M.W., van Westrenen, W., Liebske, C., 2007. Mars: A new core-
875 crystallization regime. Science 316, 1323-1325.

876 Sun, W.D., Bennett, V.C., Eggins, S.M., Kamenetsky, V.S., Arculus, R.J., 2003. Enhanced
877 mantle-to-crust rhenium transfer in undegassed arc magmas. Nature 422, 294-297.

878 Taylor, G.J., 2013. The bulk composition of Mars. Chemie der Erde - Geochemistry 73, 401-
879 420.

880 Treiman, A.H., 2005. The nakhlite meteorites: Augite-rich igneous rocks from Mars. Chemie
881 Der Erde-Geochemistry 65, 203-270.

882 Treiman, A.H., Drake, M.J., Janssens, M.J., Wolf, R., Ebihara, M., 1986. Core formation in the
883 earth and shergottite parent body (spb) - chemical evidence from basalts. Geochim. Cosmochim.
884 Acta 50, 1071-1091.

885 Usui, T., Alexander, C.M.O.D., Wang, J., Simon, J.I., Jones, J.H., 2012. Origin of water and
886 mantle–crust interactions on Mars inferred from hydrogen isotopes and volatile element
887 abundances of olivine-hosted melt inclusions of primitive shergottites. Earth and Planetary
888 Science Letters 357–358, 119-129.

889 Wänke, H., Dreibus, G., 1988. Chemical composition and accretion history of terrestrial planets.
890 Philosophical Transactions of the Royal Society A: Mathematical, Physical and Engineering
891 Sciences 325, 545-557.

892 Wadhwa, M., 2008. Redox Conditions on Small Bodies, the Moon and Mars. Reviews in
893 Mineralogy and Geochemistry 68, 493-510.

894 Wang, M.S., Mokos, J.A., Lipschutz, M.E., 1998. Martian meteorites: Volatile trace elements
895 and cluster analysis. Meteoritics & Planetary Science 33, 671-675.

Wang, Z., Becker, H., 2013. Ratios of S, Se and Te in the silicate Earth require a volatile-rich late veneer. Nature 499, 328-331.

Wang, Z., Becker, H., 2015a. Fractionation of highly siderophile and chalcogen elements during magma transport in the mantle: Constraints from pyroxenites of the Balmuccia peridotite massif. Geochim. Cosmochim. Acta 159, 244-263.

Wang, Z., Becker, H., 2015b. Abundances of Ag and Cu in mantle peridotites and the implications for the behavior of chalcophile elements in the mantle. Geochim. Cosmochim. Acta 160, 209-226.

Wang, Z., Becker, H., Wombacher, F., 2015. Mass fractions of S, Cu, Se, Mo, Ag, Cd, In, Te, Ba, Sm, W, Tl and Bi in geological reference materials and selected carbonaceous chondrites determined by isotope dilution ICP-MS. Geostand. Geoanal. Res. 39, 185-208.

Wang, Z., Laurenz, V., Petitgirard, S., Becker, H., 2016. Earth's moderately volatile element composition may not be chondritic: Evidence from In, Cd and Zn. Earth Planet. Sci. Lett. 435, 136-146.

Wasson, J.T., Kallemeyn, G.W., 1988. Compositions of Chondrites. Phil. Trans. R. Soc. A 325, 535-544.

Yang, S., Humayun, M., Righter, K., Jefferson, G., Fields, D., Irving, A.J., 2015. Siderophile and chalcophile element abundances in shergottites: Implications for Martian core formation. Meteoritics & Planetary Science 50, 691-714.

Yi, W., Halliday, A.N., Alt, J.C., Lee, D.C., Rehkamper, M., Garcia, M.O., Su, Y.J., 2000. Cadmium, indium, tin, tellurium, and sulfur in oceanic basalts: Implications for chalcophile element fractionation in the Earth. J. Geophys. Res. -Solid Earth 105, 18927-18948.

Table 1. Results of Cu, S, Se and Te contents of Martian meteorites by isotope dilution ICP-MS

Sample Name	Classification		MgO	$La/Yb_{(N)}$	$\varepsilon^{143}Nd_{(initial)}$	Mass	Cu			S			Se			Te			S/Cu		S/Se		Se/Te		Cu/Se		Cu/Te	
			(wt.%)			(g)	(μg/g)	±2s	Blank%	(μg/g)	±2s	Blank%	(ng/g)	±2s	Blank%	(ng/g)	±2s	Blank%		±2s		±2s		±2s		±2s		±2s
ALH77005	Lherzolitic shergottite	Intermediate	28	0.40	11.1	**0.1284**	**4.35**	0.09	0.7%	**712**	9	1.1%	**280**	3	0.3%	**1.02**	0.09	11%	164	4	2543	42	275	24	16	0.4	4265	387
Y-000097	Lherzolitic shergottite		26	0.35		**0.1386**	**2.65**	0.04	1.1%	**446**	7	1.7%	**132**	1	0.5%	**0.71**	0.09	15%	168	4	3379	59	186	24	20	0.3	3732	476
Sau 005	Olivine-phyric shergottite	Depleted	20	0.10	38.0	**0.0946**	**7.74**	0.09	0.6%	**1453**	15	0.8%	**397**	4	0.3%	**4.14**	0.14	4.2%	188	3	3660	53	96	3	19	0.3	1870	67
Reanalysis*							**7.76**	0.09								**4.20**	0.13											
Y-980459	*Olivine-phyric shergottite*	Depleted	19	0.12	36.9	**0.1378**	**6.49**	0.06	0.5%	**1544**	15	0.5%	**430**	4	0.2%	**5.13**	0.11	2.3%	238	3	3591	48	84	2	15	0.2	1265	30
Reanalysis*							**6.51**	0.06								**5.19**	0.12											
Tissint	Olivine-phyric shergottite	Depleted	17	0.16	44.4	**0.1471**	**9.87**	0.09	0.3%	**1997**	18	0.4%	**585**	6	0.1%	**1.19**	0.08	8.9%	202	3	3414	47	492	35	17	0.2	8294	587
EETA79001-A	Olivine-phyric shergottite	Intermediate	16	0.28	16.6	**0.1873**	**7.88**	0.07	0.3%	**1682**	15	0.3%	**411**	4	0.1%	**1.74**	0.07	5.0%	213	3	4092	54	236	10	19	0.3	4529	187
LAR06319	*Olivine-phyric shergottite*	Enriched	16	1.05	-7.2	**0.1357**	**9.07**	0.18	0.3%	**2214**	20	0.3%	**418**	4	0.2%	**2.03**	0.08	5.8%	244	5	5297	70	206	8	22	0.5	4468	197
LAR12011	Olivine-phyric shergottite	Enriched	18#			**0.1253**	**8.84**	0.18	0.4%	**1342**	13	0.6%	**327**	3	0.2%	**1.86**	0.09	6.8%	152	3	4104	55	176	9	27	0.6	4753	250
LAR12095	Olivine-phyric shergottite	Depleted	16#			**0.1781**	**7.03**	0.06	0.3%	**1919**	17	0.3%	**460**	5	0.1%	**2.88**	0.08	3.2%	273	3	4172	58	160	5	15	0.2	2441	71
Reanalysis*							**7.05**	0.06								**2.93**	0.09											
RBT04262	Olivine-phyric shergottite	Enriched	22	0.84	-6.7	**0.1659**	**4.58**	0.05	0.6%	**1940**	17	0.3%	**267**	3	0.2%	**0.67**	0.07	13%	424	6	7266	104	399	42	17	0.3	6836	718
Zagami	Basaltic shergottite	Enriched	11	0.83	-7.2	**0.1535**	**8.53**	0.08	0.3%	**1326**	13	0.5%	**307**	3	0.2%	**1.56**	0.08	6.6%	155	2	4319	60	197	10	28	0.4	5468	285
Y-000593	Nakhlite(clinopyroxenite)	Enriched	10	4.24	16.9	**0.1835**	**4.36**	0.05	0.5%	**321**	5	1.8%	**183**	2	0.3%	**0.88**	0.07	9.6%	74	1	1754	33	208	17	24	0.4	4955	398
MIL03346	Nakhlite(clinopyroxenite)	Enriched	9	3.40	16.1	**0.1553**	**10.63**	0.09	0.3%	**3860**	33	0.2%	**278**	3	0.2%	**1.30**	0.08	7.7%	363	4	13885	191	214	13	38	0.5	8177	508
Nakhla	Nakhlite(clinopyroxenite)	Enriched	12	3.69	16.2	**0.1284**	**6.03**	0.12	0.5%	**311**	7	2.6%	**74**	1	1.0%	**0.36**	0.09	27%	52	2	4203	110	206	51	81	2.0	16750	4201
ALH84001	Orthopyroxenite		25	0.46		**0.1217**	**0.09**	0.05	28%	**219**	7	3.8%	**1**	0.3	44%	**0.17**	0.09	45%											
Mean values																			171		3566		203		20		4396	
1s																			65		798		78		4		1954	
number																			n=11		n=11		n=13		n=12		n=12	

Blanks by isotope dilution	**Cu (μg)**	**S (μg)**	**Se (ng)**	**Te (ng)**
Procedual blank 1	0.003	1.5	0.11	0.018
Procedual blank 2	0.002	0.81	0.10	0.022
Procedual blank 3	0.007	0.81	0.07	0.011
Mean of blanks	**0.004**	**1.05**	**0.10**	**0.017**
2SD (n=3)	0.005	0.84	0.04	0.011
2RSD	130%	80%	40%	65%

Note: Blank% means the percentage of subtraction of total procedual blank. Reanlysis* means measurement of leftover solution of the same sample at different working days. The results show repeatable values.

The underlined ratios are not used to calculate the mean values (see text for reasons).

Y-980459 and LAR 06319 possibly are the most primtive sherogottites from the Martian mantle. Note ratios of LAR06319 are similar to the mean values, except for the elevated S by crustal input. Y-980459 shows a similar feature.

MgO contents, $La/Yb_{(N)}$ and $\varepsilon^{143}Nd_{(initial)}$ are from literature (Debaille et al., 2009; Jones, 2015; Meyer, 2013; Shirai and Ebihara, 2009). The original references for some $\varepsilon^{143}Nd_{(initial)}$ are listed in the Supplementary text. MgO with # symbol is assumed to similar to the pair of LAR06319.

Table 2. Estimated contents of S, Se and Te in the Martian mantle

Elements	Methods	Concentration in the mantle	Comments
Cu	Cu-MgO correlation	**Cu=2.0±0.4 µg/g (1s)**	Taylor (2013); This study
Se	Se/Yb ratio	Se=85±18 ng/g (1s)	Taylor (2013)
	Cu/Se ratio	**Se=100±27 ng/g (1s)**	This study; Cu/Se= 20±4
S	S/Cu ratio	Maximum S=340±140 µg/g (1s)	This study; S/Cu= 170±65
	S/Se ratio	Maximum S=360±120 µg/g (1s)	This study; S/Se= 3600±800
	S/Se ratio	Minimum S=250±70 µg/g (1s)	S/Se of different groups of chondrites are constant at 2500±400 and probably reflect similar ratio for Martian building materials. Core formation leads to no or a slight incease of S/Se in Martian mantle relative to the bulk planet.
	Recommended	**S=360±120 µg/g (1s)**	The possible maximum and minimum values are simialr with uncertainty
Te	Cu/Te ratio	Te=0.45±0.23 ng/g (1s)	This study; Cu/Te = 4400±2000
	Se/Te ratio	Te=0.50±0.25 ng/g (1s)	This study; Se/Te = 200±80
	Y-980459 data	Maximum Te=1.2-1.5 ng/g	Y-980459 has the lowest ratios of Se/Te=84 and Cu/Te=1265. The maximum value does not change the conclusion of a low Te content in the Martian mantle.
	Recommended	**Te=0.50±0.25 ng/g (1s)**	

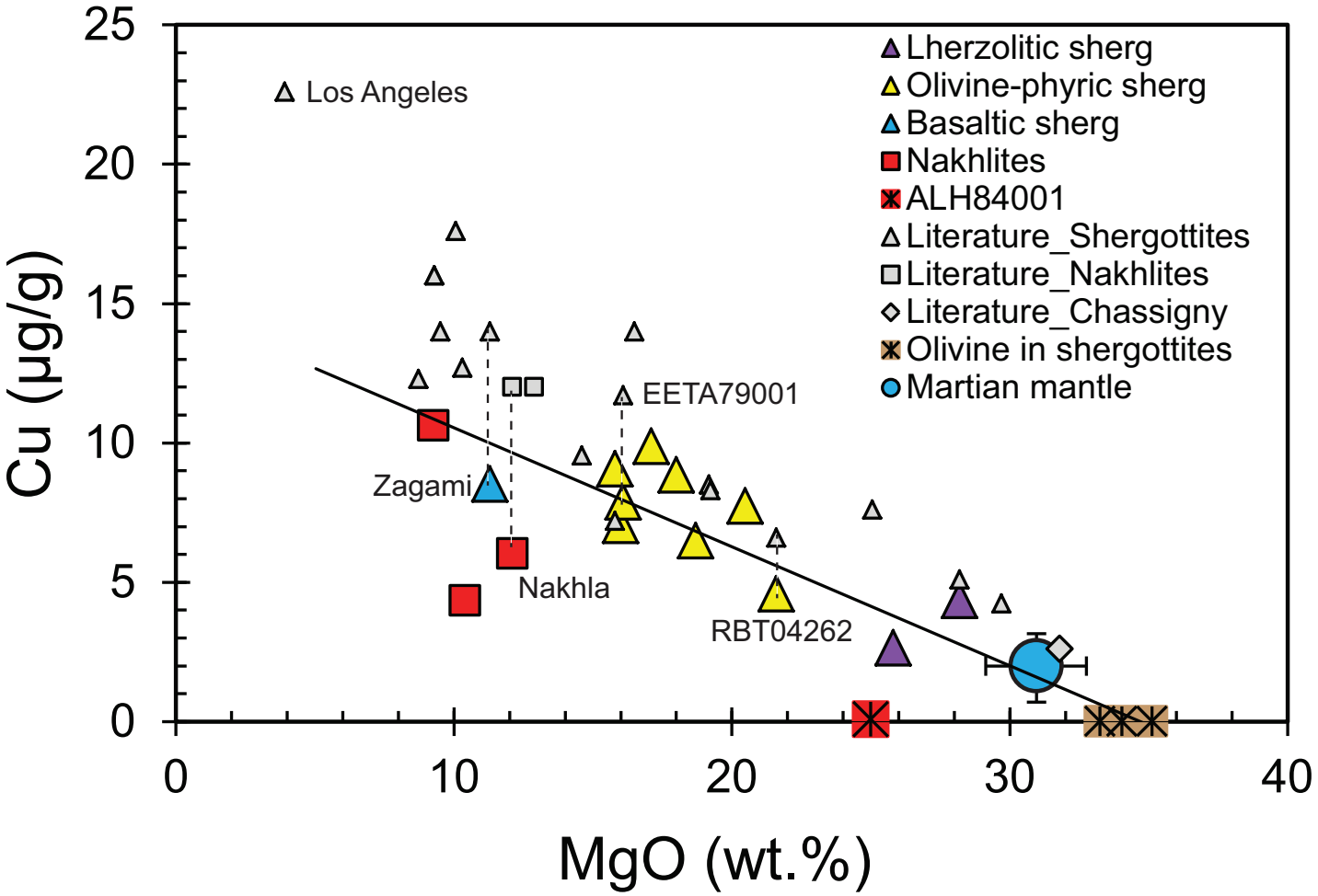

Figure 1 Cu-MgO

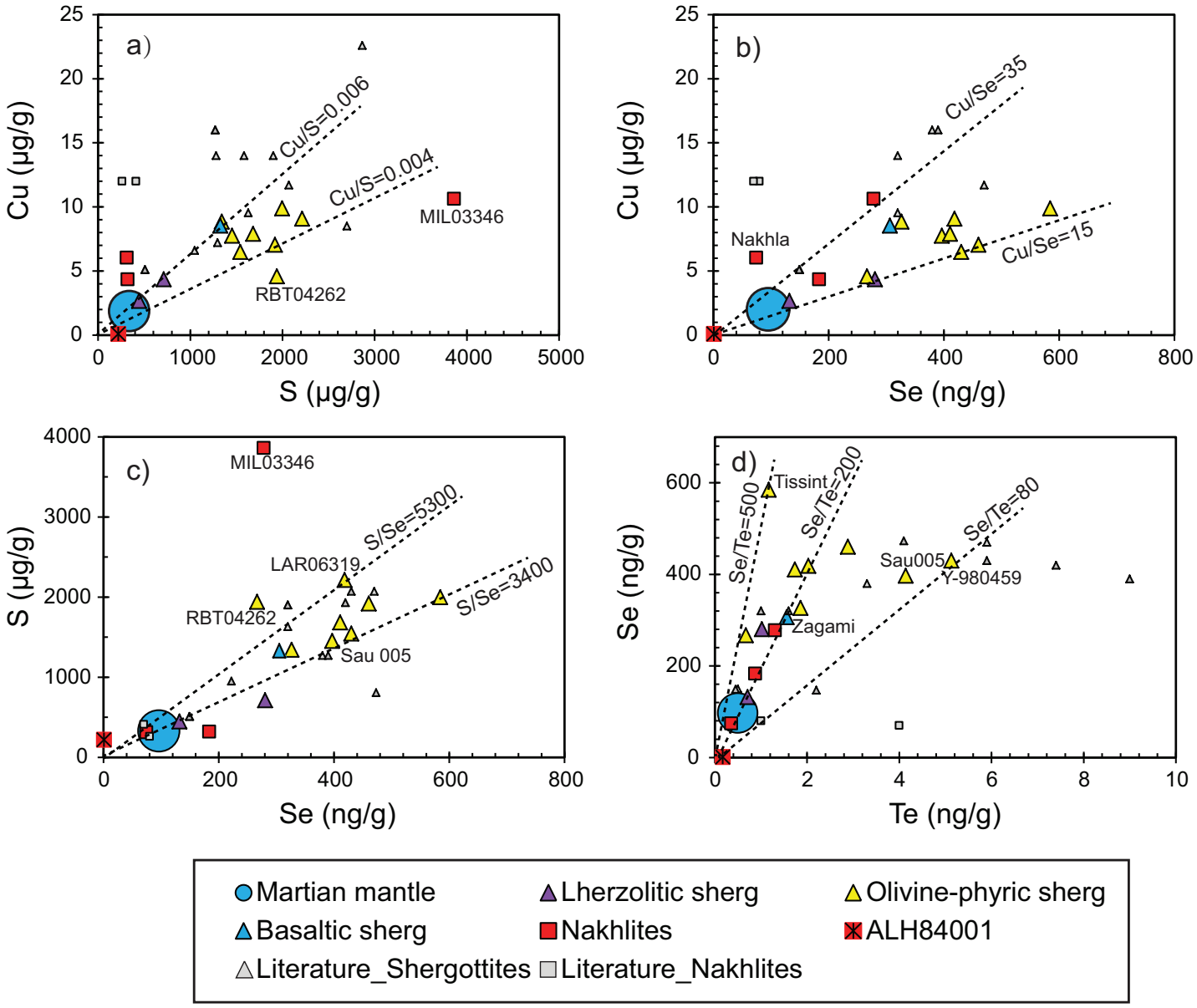

Figure 2 element pairs

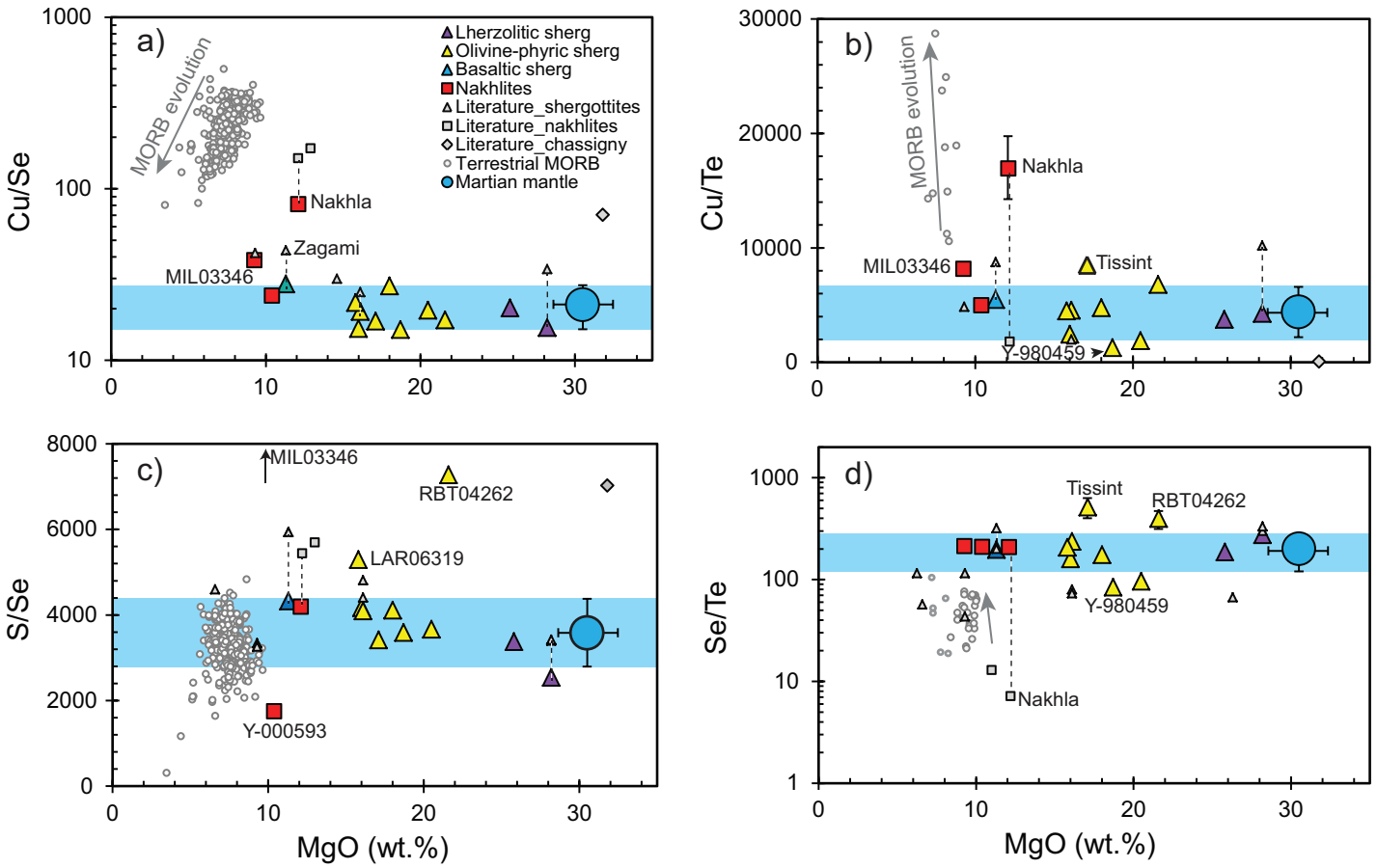

Figure 3 Ratios of Cu S Se Te - R1

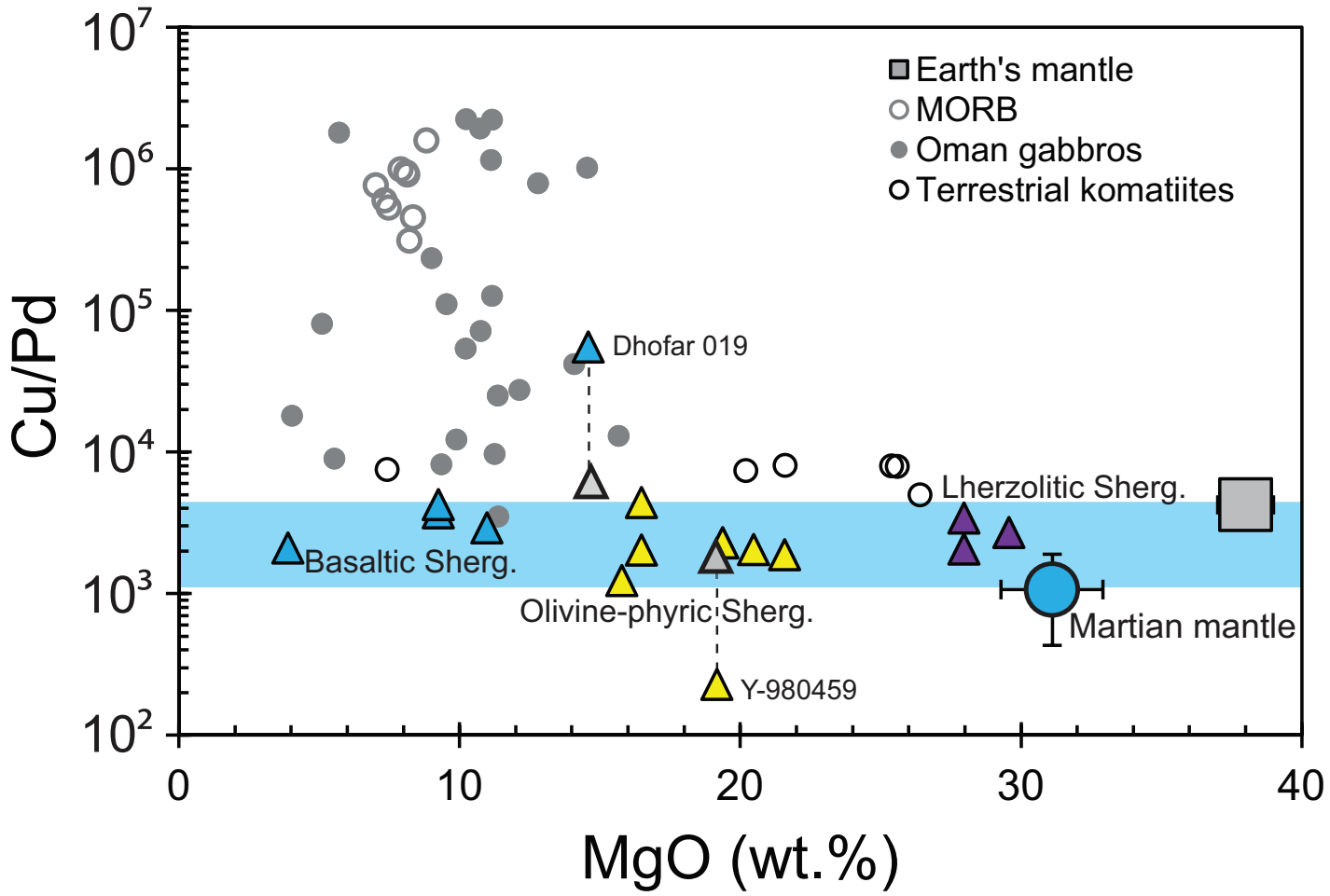

Figure 4 Cu-Pd ratios_R1

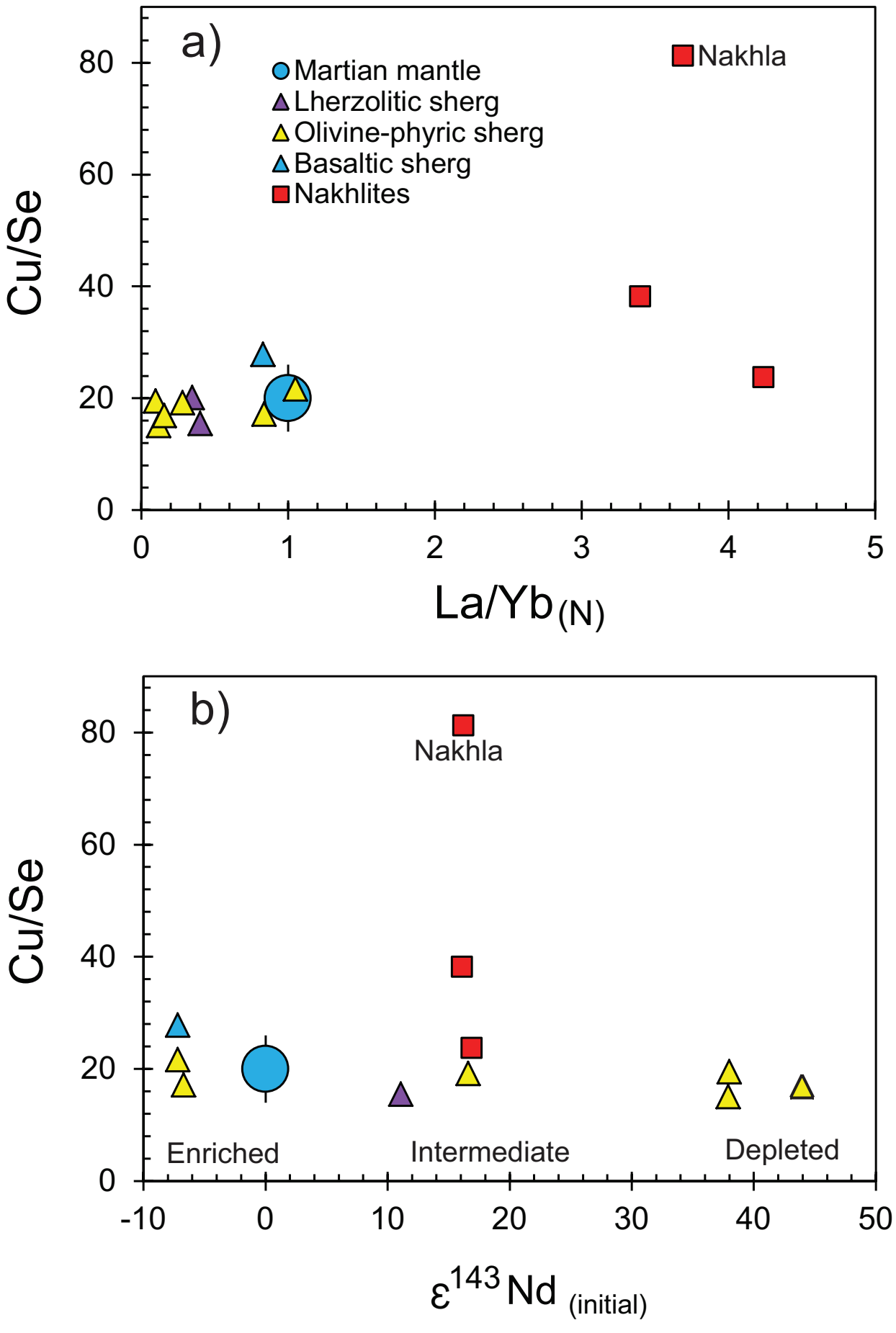

Figure 5 Cu-Se ratio versus Nd isotopes

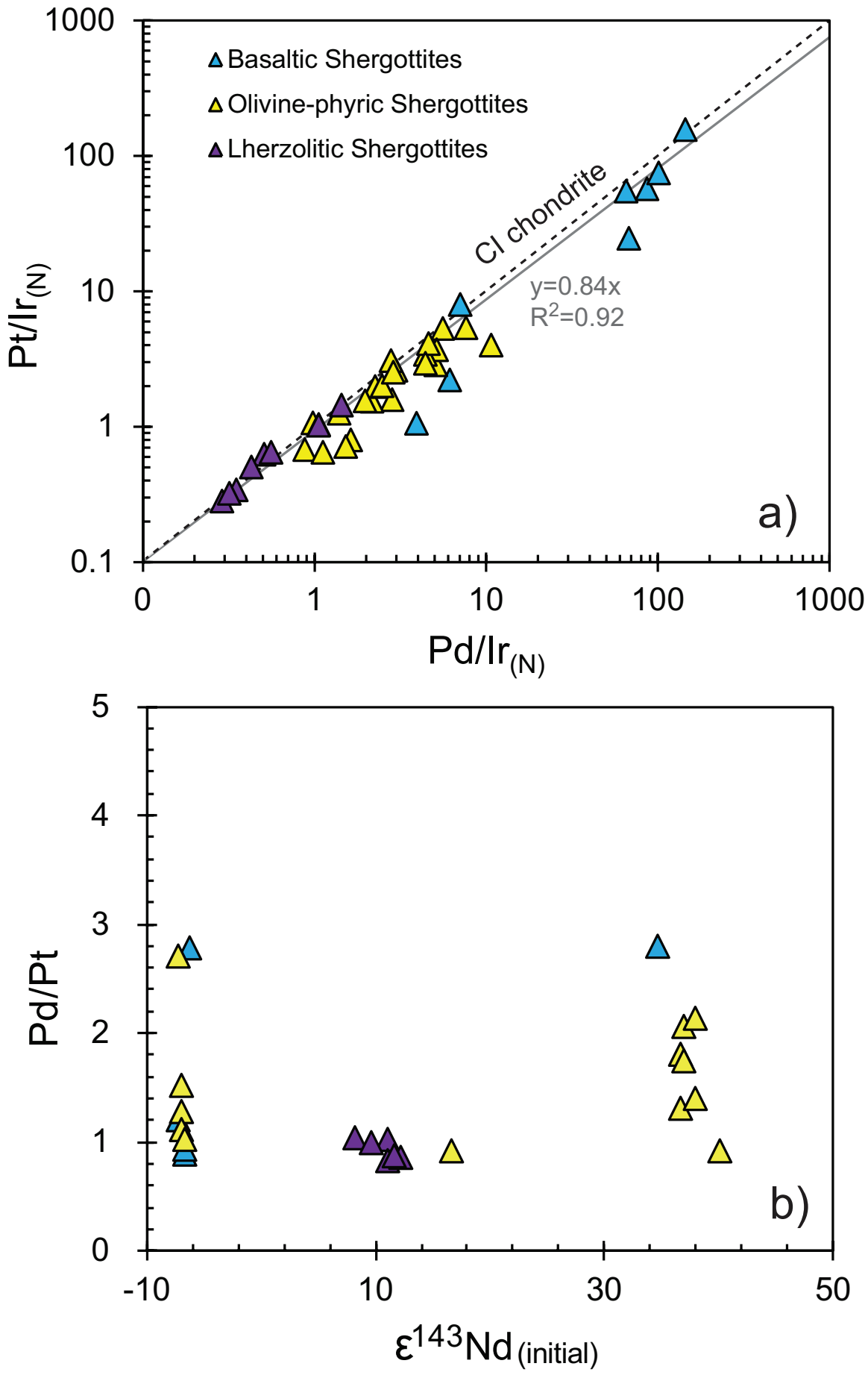

Figure 6 PGE ratios R1

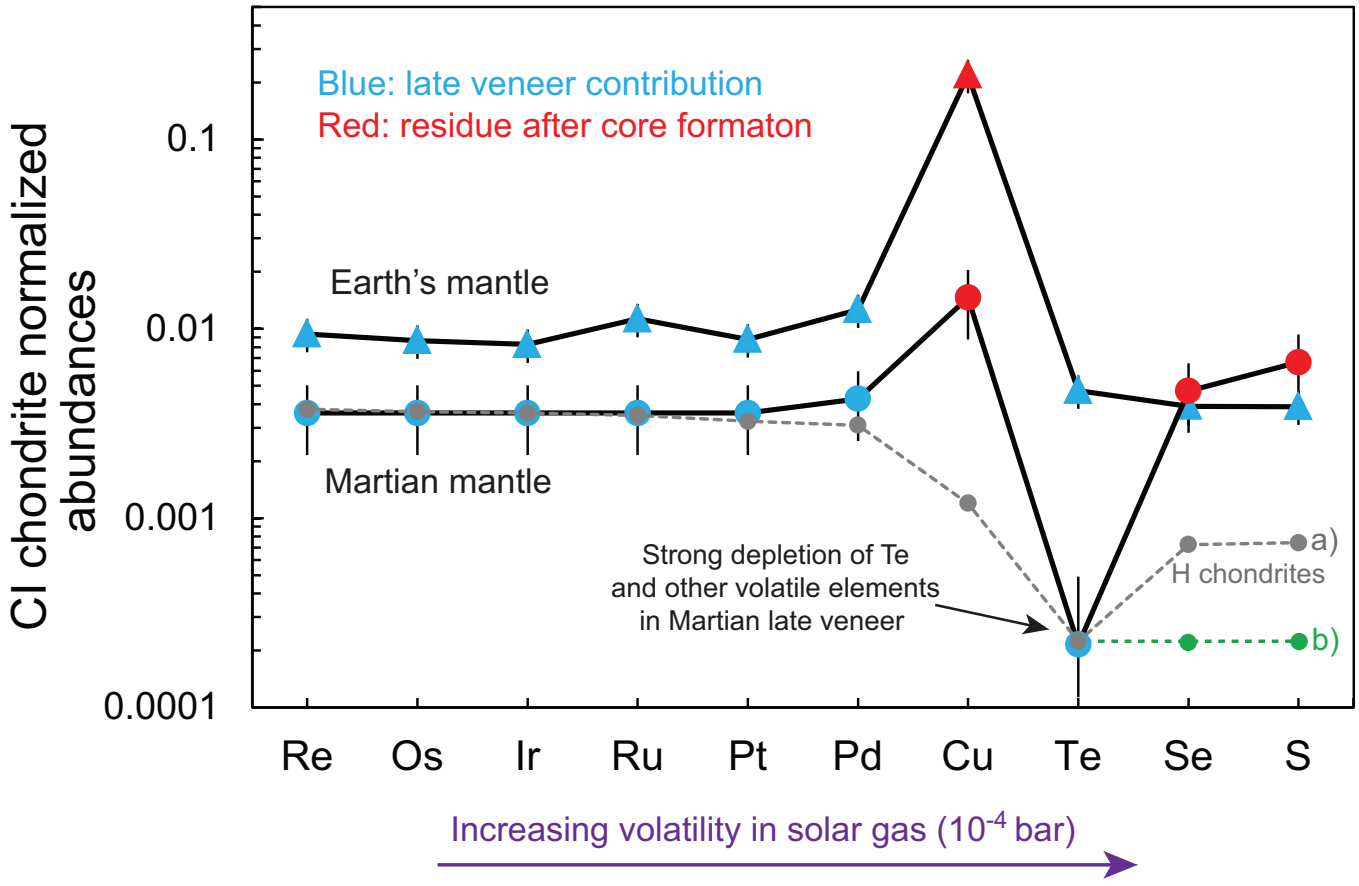

Figure 7 Late veneer compositions updated

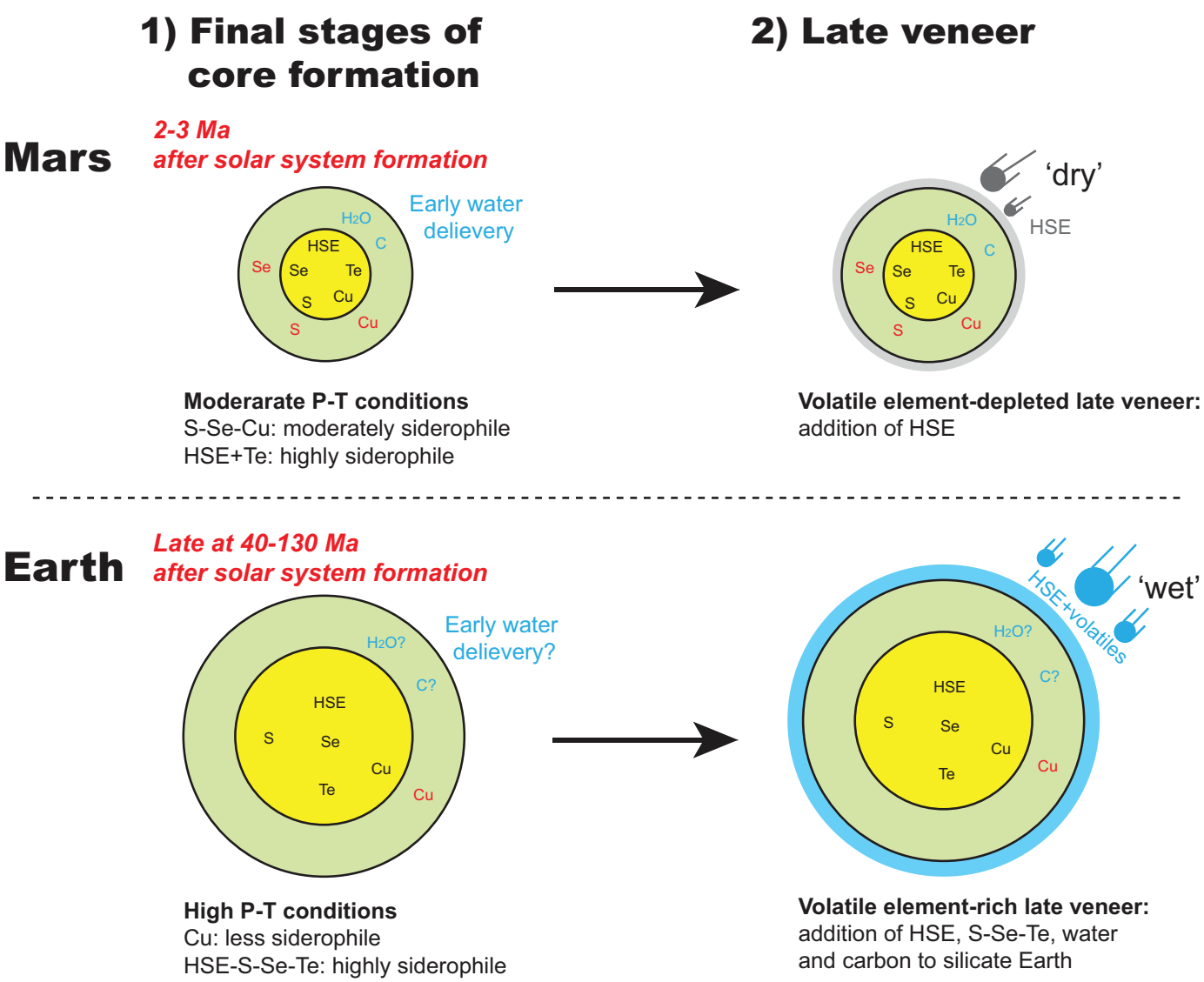

Figure 8 cartoon